



# Silicate–natrocarbonatite liquid immiscibility in 1917 eruption combeite–wollastonite nephelinite, Oldoinyo Lengai Volcano, Tanzania: Melt inclusion study

Victor V. Sharygin <sup>a,\*</sup>, Vadim S. Kamenetsky <sup>b</sup>, Anatoly N. Zaitsev <sup>c,d</sup>, Maya B. Kamenetsky <sup>b</sup>

<sup>a</sup> V.S. Sobolev Institute of Geology and Mineralogy SB RAS, Koptyuga prospect 3, Novosibirsk 630090, Russia

<sup>b</sup> ARC Centre of Excellence in Ore Deposits and School of Earth Sciences, University of Tasmania, Hobart, Tasmania 7001, Australia

<sup>c</sup> Department of Mineralogy, Faculty of Geology, St. Petersburg State University, University Emb. 7/9, St. Petersburg 199034, Russia

<sup>d</sup> Department of Mineralogy, Natural History Museum, Cromwell Road, London, SW7 5BD UK

## ARTICLE INFO

### Article history:

Received 15 October 2011

Accepted 24 January 2012

Available online 2 February 2012

### Keywords:

Melt inclusions

Peralkaline glasses

Silicate–carbonate liquid immiscibility

Combeite wollastonite nephelinite

Natrocarbonatite

Oldoinyo Lengai

## ABSTRACT

Primary silicate–melt and carbonate–salt inclusions occur in the phenocrysts (nepheline, fluorapatite, wollastonite, clinopyroxene) in the 1917 eruption combeite–wollastonite nephelinite at Oldoinyo Lengai. Silicate–melt inclusions in nepheline clearly show liquid immiscibility phenomena expressed in the presence of carbonate globules in silicate glass. The coexistence of inclusions with markedly different proportions of silicate glass + vapor–carbonate globule in the core of nepheline phenocrysts, the presence of carbonate–salt inclusions in fluorapatite and our heating experiments strongly suggest that their entrapment began at temperatures higher than 1130 °C in an intermediate chamber when initial carbonated nephelinite melt was heterogeneous and represented a mixture of immiscible liquids. Silicate–natrocarbonatite melt immiscibility took place at high temperature and immiscible nephelinite and carbonatite liquids coexisted over a wide temperature range from  $\geq 1130$  °C to 600 °C. Homogenization of a carbonate globule (dissolution of the gas bubble in carbonate melt) at 900–940 °C indicates that after separation from silicate magma the natrocarbonatite represented homogeneous liquid in the 900–1130 °C temperature range, whereas below these temperatures immiscible melts of different composition and fluid phase have separated from it. The bulk composition of homogeneous natrocarbonatite melt may be estimated as  $\approx 20\%$  CaF<sub>2</sub>, 40–60% (Na, K)<sub>2</sub>CO<sub>3</sub> and 20–40% CaCO<sub>3</sub> based on the coexistence of nyerereite, calcite and fluorite and the rapid phase transition (carbonate aggregate → carbonate liquid) at 550–570 °C observed in vapor–carbonate globules of nepheline-hosted silicate–melt inclusions and on the Na<sub>2</sub>CO<sub>3</sub>–CaCO<sub>3</sub>–CaF<sub>2</sub> phase diagram. Silicate glasses of nepheline-hosted immiscible inclusions drastically differ from host nephelinite in the abundance of major and trace elements. They are high peralkaline ((Na + K)/Al – up to 9.5) and virtually free of water (H<sub>2</sub>O < 0.6 wt.%). Their very high Zr/Hf and Nb/Ta ratios and Li contents indicate that these silicate glasses represent the most evolved compositions at Oldoinyo Lengai. The peralkaline character of nephelinite melt is expressed in the composition of the daughter mineral assemblage within silicate–melt inclusions in nepheline (delhayelite, leucite, mica, clinopyroxene). These minerals show strong deficiency in Al and enrichment in Fe<sup>3+</sup> that is also common to the groundmass of the Oldoinyo Lengai combeite–wollastonite nephelinites.

© 2012 Elsevier B.V. All rights reserved.

## 1. Introduction

Oldoinyo Lengai is the only active volcano on the Earth erupting natrocarbonatite lava. This provides a unique opportunity to study these “ephemeral” rocks because they are very quickly degraded under atmospheric conditions (Dawson, 1962; Zaitsev and Keller, 2006; Zaitsev et al., 2008). Several types of peralkaline magmas are involved in the evolution of Oldoinyo Lengai: olivine melilitite, phonolite, nephelinite and natrocarbonatite (Donaldson et al., 1987; Keller et al., 2006; Klaudius and Keller, 2006). Geological observations strongly suggest

liquid immiscibility relationships between nephelinite and natrocarbonatite at Lengai (Dawson, 1962; Dawson et al., 1996; Keller and Krafft, 1990). Despite numerous publications the petrogenesis of different carbonatites, and natrocarbonatites in particular, is far from total solution. The study of silicate and carbonate melt inclusions trapped by minerals gives additional information to better understand the relationships between silicate and carbonatite melts, and PT-conditions of their formation. Recently melt inclusions have been routinely used in the studies of carbonatites and related rocks (e.g., Rankin and Le Bas, 1974 and references therein; Golovin et al., 2007; Guzmics et al., 2011; Kamenetsky et al., 2007; Mitchell, 2009; Mitchell and Dawson, 2012–this volume; Panina, 2005; Sharygin et al., 2011; Stoppa et al., 1997, 2009; Veksler et al., 1998; Zaitsev, 2010b; Zaitsev et al., 2011, 2012–this volume).

\* Corresponding author. Tel.: +7 383 3333608; fax: +7 383 3332792.

E-mail address: [sharygin@igm.nsc.ru](mailto:sharygin@igm.nsc.ru) (V.V. Sharygin).

This paper presents detailed data on silicate melt inclusions in minerals in a combeite–wollastonite nephelinite (CWN) lava flow from Oldoinyo Lengai, erupted in the period 1904–1917 (Dawson et al., 1995a, 1995b; Keller et al., 2010). The exact time of eruption for this lava flow is unknown. However, the 1917 eruption was the most powerful event in the above period and considerable volumes of nephelinite lava and pyroclastics were emitted (Keller et al., 2010). The unpublished data of J. Keller (personal communication) clearly proves that this lava flow is related to the 1917 eruption. For the sake of convenience, the flow will be referred to hereafter as “the 1917 flow”. The main emphasis is on their mineralogy, major and trace element composition, and heating experiments of nepheline-hosted inclusions. These data, especially heating experiments, provide a unique opportunity to follow in situ behavior of coexisting silicate and natrocarbonatite melts during the liquid immiscibility process(es). Other publications on melt inclusions at Oldoinyo Lengai have been concerned only with the compositional features of immiscible components (Mitchell, 2009; Mitchell and Dawson, 2012-this volume) or homogenization temperatures (Naumov et al., 1972).

## 2. Position and stratigraphy of Oldoinyo Lengai

Oldoinyo Lengai is located in the eastern branch of the East African Rift System, south of Lake Natron (Dawson, 2008; Keller et al., 2006; Klaudius and Keller, 2006) and close to the ca. 400 m high escarpment of the Gregory Rift, which formed 1.2 Ma ago (Foster et al., 1997; MacIntyre et al., 1974). The timing of the onset of volcanic activity at Oldoinyo Lengai is constrained with an age of 0.37 Ma for pyroclastic rocks underlying the “yellow tuffs and agglomerates” (Bagdasaryan et al., 1973; MacIntyre et al., 1974). The historical activity of Oldoinyo Lengai, with observations covering about last 100 years (since 1904), was summarized by Dawson et al. (1995a, 1995b) and Keller et al. (2010).

Dawson (1962) first established the stratigraphy of Oldoinyo Lengai, which was re-iterated by Klaudius and Keller (2006) defining the following major structural units: Lengai I – phonolite tuffs and phonolite lavas; Lengai II A – nephelinite tuffs and nephelinite lavas; Lengai II B: nephelinite tuffs, nephelinite lavas, gray melilite-bearing nephelinite tuffs and carbonatite tuffs and lavas of the active northern crater. Phonolites and phonolitic nephelinites are dominant in the early activity from the now-extinct southern crater that formed the major bulk of the volcano (Lengai I), whereas nephelinites of Lengai II characterize silicate fraction of the pyroclastic rocks and lavas from the northern crater. Lengai I forms approximately 60% of the volcano's volume, Lengai II ~35% of which natrocarbonatites are subordinate with less than 5% (Klaudius and Keller, 2006). In addition, some parasitic cones and lava flows (e.g., Nasira, Dorobo) located on the slopes of the volcano are closely related to the Lengai II activity (Keller et al., 2006).

## 3. Experimental and analytical techniques

Phenocrysts and microphenocrysts (nepheline, fluorapatite, wollastonite, and clinopyroxene) containing silicate melt inclusions and coexisting fluid and crystal inclusions were carefully selected from doubly polished rock thin sections and individual mineral grains, which were specially handpicked from different fractions of crushed rock.

Experimental studies on individual melt inclusions were performed in an argon atmosphere using a high-temperature heating stage (up to 1600 °C) with visual monitoring technique developed by Sobolev and Slutsky (1984) and installed at the Institute of Geology and Mineralogy (IGM), Novosibirsk, Russia. This technique was used to evaluate homogenization temperatures for melt inclusions and ranges of melting for daughter phases. Part of the microthermometric experiments was undertaken at the University of Tasmania (UT), Hobart, Australia using the Linkam TS1500 heating stage.

Electron microprobe analysis (EMPA-WDS) of rock-forming minerals and solid phases of the silicate melt inclusions was mainly performed at the IGM using a Camebax 50X electron microprobe (accelerating voltage 20 kV, probe current 15–30 nA, focused beam size 2–3 μm, measuring time for each element 40 s). Natural minerals and synthetic compounds close in composition to analyzed phases were used as standards: albite (Na), orthoclase (K, Al), diopside and wollastonite (Mg, Ca, Si), chlorapatite (P, Cl), ilmenite (Ti), fluorophlogopite (Mg, Al, Si, F), zircon (Zr), spessartine (Mn), pyrope and hematite (Fe), LiNbO<sub>3</sub> (Nb), Ba- and Sr-rich silicate glasses (Ba, Sr), and barite (Ba, S). Precisions for major and minor elements were better than 2 and 5 rel.%, respectively. Data reduction was performed using a PAP routine. Overlap corrections were done for the following elements: Ti–Kα–Ba–Lα; Si–Kα–Sr–Lα; Fe–Lα–F–Kα.

Melt inclusions were exposed in the polished rock fragments and individual grains were prepared using water-free Al<sub>2</sub>O<sub>3</sub> and diamond powders to prevent loss of water-soluble components or hydration of phases.

For other petrographic studies, phase identification and EDS-qualitative analysis, BSE-imaging and elemental mapping we used Leo 1430VP EDX Oxford and JEOL JSM-35 scanning electron microscopes at the IGM, and a FEI Quanta-600 scanning electron microscope at the UT operated at 20–25 kV and 1 nA.

The trace-element composition of glasses from nepheline-hosted melt inclusions was obtained by secondary-ion mass spectroscopy (SIMS) on a Cameca IMS-4f ion probe at the Institute of Physics and Technology, Yaroslavl Branch in Yaroslavl, Russia. For analysis, inclusions larger than 20 μm and previously analyzed by EMPA were selected. Analysis of trace elements (Be, Li, B, Cr, V, Rb, Ba, Th, U, Nb, Hf, Sr, Zr, Y, REE) and Ti was carried out by the energy filter method; operating conditions: primary O<sup>2-</sup> beam – 20 μm, *I* = 2–4 nA, energy offset – 100 eV, and energy slit – 50 eV. Concentrations of elements and water were determined from the ratios of their isotopes to <sup>30</sup>Si, using calibration curves for standard samples (Jochum et al., 2000). Low background contents of H<sub>2</sub>O (0.03 wt.%) by the mass spectrometer was possible due to the 24 h high-vacuum exposure of the samples. The NIST610 glass was used as a standard.

Qualitative trace-element concentrations in the largest near-surface non-opened inclusions (>20 μm) in nepheline phenocrysts were established by laser-ablation-inductively coupled plasma-mass spectrometry (LA-ICP-MS) at the UT. This instrumentation consists of a New Wave Research UP213 Nd–YAG (213 nm) laser coupled to an Agilent 4500 quadrupole mass-spectrometer. For this study, analyses were performed in a He atmosphere by ablating spots of 8–15 μm in diameter at a rate of 5–10 pulses/s using a laser power of ~10 J/cm<sup>2</sup>.

## 4. Sample petrography

The studied sample (OL 7/2000) was collected from a lava flow that occurs on the western rim of the northern crater (see Fig. 1 in Zaitsev et al. (2008)). This outcrop is shown on the map of Dawson (1962) and samples from the outcrop (BD119, WCN119 and OL-7) have been described in Donaldson et al. (1987), Dawson (1998) and Keller and Krafft (1990). After the 2007–2008 explosive eruptions this outcrop, like the rest of the upper slopes of the mountain, is now completely buried by a carbonate–silicate ash (Keller et al., 2010; Kervyn et al., 2010; Mattsson and Reusser, 2010; Mitchell, 2009; Mitchell and Dawson, 2007). The studied sample is a combeite-bearing nephelinite (Keller and Krafft, 1990; Keller and Spettel, 1995) and later was labeled as Lengai IIB CWN (Klaudius and Keller, 2006). It is porphyritic, greenish gray in color and contains numerous vesicles. Abundant euhedral phenocrysts (1–5 mm) comprise mainly nepheline and clinopyroxene, and rarely wollastonite, combeite, Ti-bearing andradite to schorlomite, titanite, and fluorapatite. The groundmass consists of microphenocrysts (<1 mm) and

microlites of the above mentioned minerals and green to brown glass. The proportion of phenocrysts and microphenocrysts is approximately 50%. Delhayelite, perovskite, magnetite, pyrrhotite, sodalite, K-feldspar, Sr-bearing baryte, unidentified K–Na–Ba–Ti–Fe-silicate (possibly, a Fe<sup>3+</sup>-rich intermediate member of the shcherbakovite–noonkanbahite–batisite series, Uvarova et al., 2010), galena and calcite are minor and accessory minerals in the groundmass. Abundant vesicles contain faceted crystals of all primary minerals and are sometimes filled with secondary scalenohedral calcite and/or zeolites. Combeite coronas are common on wollastonite phenocrysts and microphenocrysts. The latter mineral is represented by the 1 T polytype: a = 7.9255 Å, b = 7.3237 Å, c = 7.0623 Å, α = 90.021, β = 95.252, γ = 103.362, space group P-1. No carbonate globules are found in the groundmass glass unlike in a combeite nephelinite from the Nasira parasitic cone (Mitchell and Dawson, 2012-this volume). Alteration is insignificant but is shown by (i) partial replacement of combeite by apophyllite (?), (ii) pyrrhotite by Fe-hydroxides, (iii) in the occurrence of a hydrated rim (hydrodelhayelite?) around delhayelite and (iv) in color changes in the groundmass glass from green to brown.

In general, the studied rock is similar to combeite–wollastonite nephelinite previously described by Dawson (1998), Dawson and Hill (1998), and Klaudius and Keller (2006). Representative analyses of minerals and groundmass glass in the studied CWN are given in Table 1.

**5. Petrography of melt inclusions in phenocrysts**

The melt inclusions are most common in nepheline phenocrysts, although, they rarely occur in nepheline microphenocrysts. Scarce melt inclusions were found in fluorapatite, wollastonite and clinopyroxene phenocrysts and microphenocrysts.

**5.1. Nepheline**

Primary silicate melt inclusions (10–100 μm) sometimes together with crystal inclusions outline the growth zones in host nepheline phenocrysts (Fig. 1). Other primary inclusion types (fluid, carbonate,

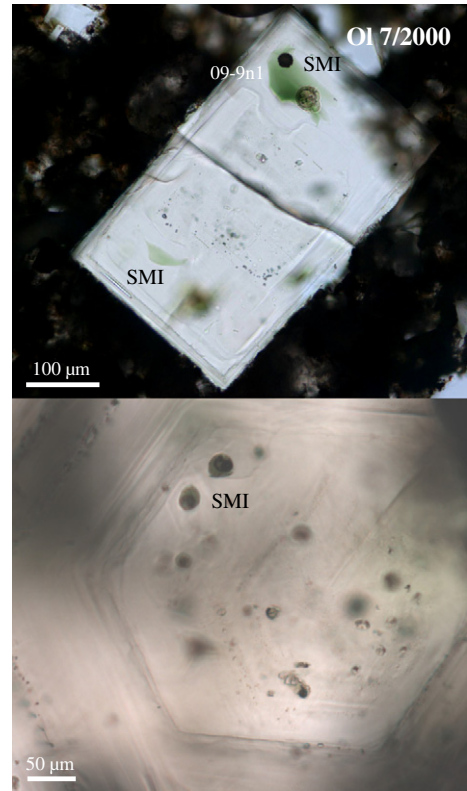


**Fig. 1.** Silicate–melt inclusions (SMI) decorate growth zones in nepheline phenocrysts, sample OI 7/2000, CWN, Oldoinyo Lengai. Number near an inclusion refers to data in Table 4.

sulfide and chloride) are scarce. Diopsidic clinopyroxene is abundant among crystal inclusions in nepheline, whereas other crystallites (fluorapatite, titanite, Ti-andradite, magnetite and perovskite) occur occasionally. Trails of secondary melt inclusions cross-cutting nepheline grains are also rare. The central zones of some nepheline

**Table 1**  
Representative analyses of minerals in CWN IIB, sample OI 7/2000, Oldoinyo Lengai.

wt.%	Ne			Cpx			Ap	Wo	Cmb	Tnt	Gr	Gr	Dlh	Dlh	Gl	Gl										
	ph	gm	r	mph													ph	ph	crn	in Ne	gm	gm	gm	gm	gm	gm
	c	c		c	m	r											c	c				c	c			
SiO <sub>2</sub>	42.38	42.92	42.94	49.38	49.93	51.15	0.65	51.18	51.05	29.43	31.48	26.77	44.72	43.98	44.40	46.06										
TiO <sub>2</sub>	0.00	0.00	0.00	1.49	0.52	0.52	0.00	0.02	0.00	38.69	9.62	18.97	0.43	0.43	3.13	2.48										
ZrO <sub>2</sub>								0.00	0.00	0.38	0.19				0.00											
Nb <sub>2</sub> O <sub>5</sub>								0.00	0.00	0.78	0.00				0.10											
Al <sub>2</sub> O <sub>3</sub>	32.52	31.31	31.22	2.90	1.07	0.86	0.00	0.00	0.00	0.59	0.65	0.14	2.84	5.11	2.16	2.76										
Fe <sub>2</sub> O <sub>3</sub>	1.83	2.98	3.23	5.68	10.98	7.70		0.55		22.30	16.54	7.27	4.45													
FeO				5.69	11.51	9.01	0.02	0.48	0.99	1.88	3.11	4.13			20.24	17.84										
MnO	0.00	0.00	0.00	0.25	0.65	0.45	0.05	0.40	0.47	0.00	0.40	0.30	0.25	0.09	0.89	0.87										
MgO	0.05	0.09	0.11	11.28	4.73	8.24	0.02	0.15	0.28	0.02	0.53	0.84	0.66	0.58	1.19	1.08										
CaO	0.05	0.09	0.06	22.39	17.24	19.59	55.66	46.63	25.66	26.85	31.23	30.73	12.87	14.30	0.24	0.86										
BaO	0.00	0.00	0.00	0.00	0.00	0.00	0.00	0.00	0.00	0.11	0.00	0.00	0.57	0.08	2.03	2.15										
SrO								0.02	0.33	0.06	0.00				0.40											
Na <sub>2</sub> O	15.22	14.83	14.89	1.22	3.77	2.67	0.21	0.07	21.17	0.14	0.42	0.81	6.19	6.77	5.58	7.28										
K <sub>2</sub> O	8.13	8.14	8.09	0.00	0.00	0.00	0.01	0.00	0.05	0.14	0.00	0.00	18.77	18.59	7.26	9.31										
P <sub>2</sub> O <sub>5</sub>	0.00	0.00	0.00	0.00	0.00	0.00	39.17	0.00	0.00	0.00	0.00	0.00	0.00	0.00	0.58	0.49										
F	0.00	0.00	0.00	0.00	0.00	0.00	2.03			0.47		0.00	4.68	4.16		0.62										
Cl	0.00	0.00	0.00	0.00	0.00	0.00	0.01	0.00	0.00	0.00	0.00	0.00	3.06	4.35	0.61	0.02										
SO <sub>3</sub>	0.00	0.00	0.00	0.00	0.00	0.00	0.04	0.00	0.00	0.00	0.00	0.00	0.62	0.25	6.06	4.52										
Total	100.18	100.36	100.54	100.28	100.40	100.19	97.87	99.50	100.00	99.54	99.93	99.23	102.93	103.14	94.87	96.34										
O = (F, Cl) <sub>2</sub>	0.00	0.00	0.00	0.00	0.00	0.00	0.86	0.00	0.00	0.20	0.00	0.00	2.66	2.73	0.14	0.26										
Total	100.18	100.36	100.54	100.28	100.40	100.19	97.01	99.50	100.00	99.34	99.93	99.23	100.27	100.41	94.73	96.07										

Fe<sub>2</sub>O<sub>3</sub> and FeO are calculated from charge balance.  
 Symbols: Ne – nepheline; Cpx – clinopyroxene; Ap – fluorapatite; Wo – wollastonite; Cmb – combeite; Tnt – titanite; Gr – Ti-rich garnet; Dlh – delhayelite; Gl – groundmass silicate glass; ph – phenocryst; mph – microphenocryst; gm – groundmass; crn – corona around wollastonite; c, m, r – core, intermediate zone and rim of grain.

phenocrysts contain very abundant inclusions (silicate melt, crystal, etc.), whereas only single inclusions occur in the outer zones.

Silicate melt inclusions in nepheline are rounded, oval or irregular in the shape and clearly show liquid immiscibility phenomena expressed in the presence of carbonate or a unified vapor-carbonate globule in silicate glass (Figs. 1 and 2). In general the phase composition of inclusions varies from glassy (green glass + gas bubble + carbonate globule (or vapor-carbonate globule(s)) ± trapped crystals) to partly crystallized (green glass + gas bubble or vapor-carbonate globule + daughter silicate crystals ± fluorite) and even to pure carbonate (vapor-carbonate globule + small amount of silicate glass) (Figs. 2 and 3). The most typical glassy inclusions contain silicate glass and one vapor-carbonate globule. In some inclusions gas and carbonate components are separated into individual phases, and the gas bubbles always contain some precipitate (salt crystals) on the walls (Fig. 2). In the majority of glassy inclusions the ratio of silicate glass to carbonate + gas is constant (approximately 60:40). However, in carbonate-rich inclusions this ratio is down to 30:70 and even 10:90. According to optical observations, SEM and EMPA, accidentally trapped crystals in glassy inclusions are diopside, fluorapatite, Ti-andradite and titanite, whereas daughter phases in partly crystallized inclusions are represented by zoned aegirine-rich clinopyroxene, Fe-rich leucite and delhayelite, brown Fe-rich mica, fluorite, wollastonite and K-feldspar (Fig. 3). Daughter fluorite may occur both in the carbonate globule and in silicate glass (Figs. 2 and

3). It should be noted that partly crystallized and carbonate inclusions are most common in the core of nepheline phenocrysts.

The carbonate globule is commonly represented by a fine-grained aggregate (Figs. 2 and 3), in which some individual phases (calcite, nyerereite, Na-carbonate, fluorite, Ca-Mg-Fe-carbonate, alkali chlorides and sulfates, SEM-EDS data) are present, similar to gregoryite-hosted inclusions from the Oldoinyo Lengai natrocarbonatite (Mitchell and Belton, 2004). Some of them show quenched dendritic texture as in the immiscible nepheline-hosted inclusions from the Oldoinyo 2007–2008 eruptions (Mitchell, 2009). However, some globules in our inclusions are optically zoned (Fig. 2) with possible enrichment of a particular zone by one mineral, whereas single carbonate globules without gas bubbles look optically homogeneous suggesting monomineralic composition.

In addition to Oldoinyo Lengai, immiscible melt inclusions were previously described in nephelinite lavas of other carbonatite-related volcanoes of the Gregory rift (Bazarova et al., 1975; Rankin and Le Bas, 1974; Romanchev, 1972; Zaitsev et al., 2011, 2012–this volume).

## 5.2. Other minerals

In addition to nepheline, rare melt inclusions were found in fluorapatite, wollastonite and clinopyroxene phenocrysts and microphe-nocrysts of the studied CWN. Wollastonite-hosted inclusions (5–20 μm) consist of silicate glass (or fine devitrified aggregate) and

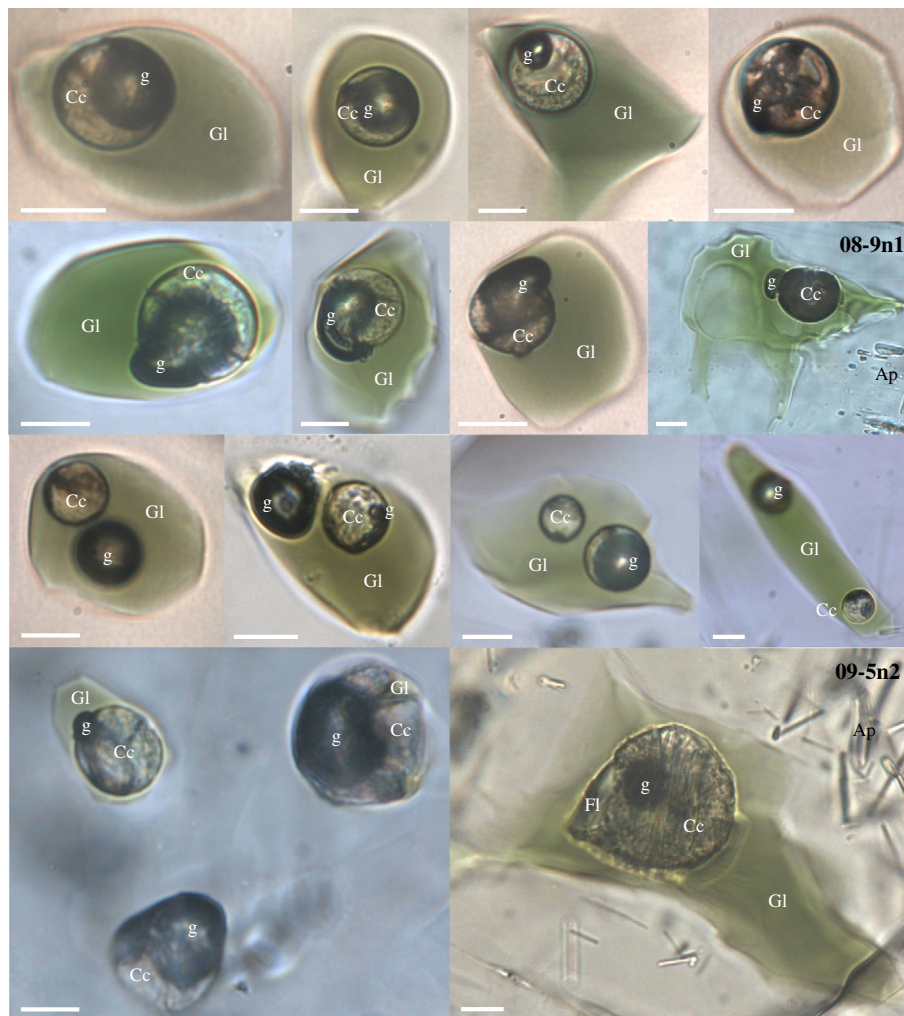


**Fig. 2.** Variable relationships between gas and natrocarbonatite in silicate–melt inclusions without daughter silicate minerals, nepheline phenocrysts, sample OI 7/2000, CWN, Oldoinyo Lengai. Scale bar is 10 μm. Inclusions with numbers refer to data in Tables 4 and 6. Symbols: Gl – silicate glass; g – gas bubble; Cc – natrocarbonatite aggregate; Ap – fluorapatite; Fl – fluorite.

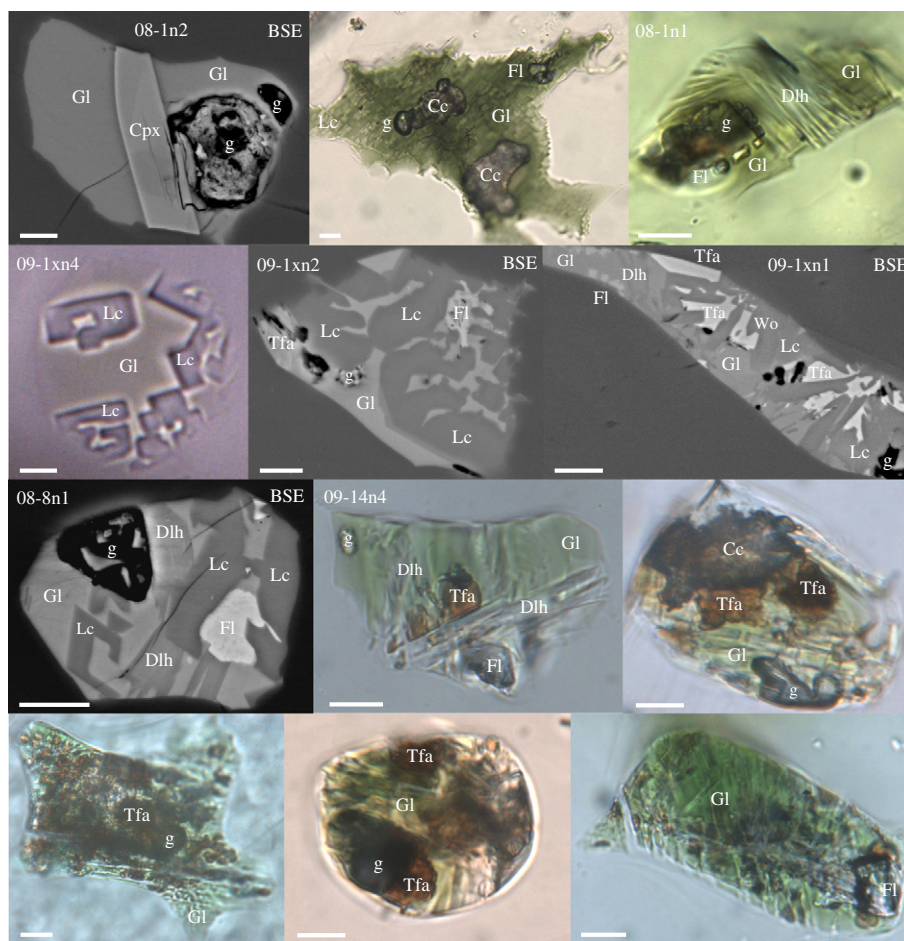


**Fig. 3.** Partly crystallized silicate–melt inclusions in nepheline phenocrysts, sample Ol 7/2000, CWN, Oldoinyo Lengai. Scale bar is 10  $\mu\text{m}$ . Inclusions with numbers refer to data in Tables 2, 3, 5, and 6. Symbols: Cpx – clinopyroxene; Dlh – delhayelite; Lc – leucite; Tfa – tetraferriannite; Wo – wollastonite. Other abbreviations see Fig. 2.

a gas bubble. Silicate melt inclusions in clinopyroxene (20–100  $\mu\text{m}$ ) are completely crystallized and contain daughter phases (wollastonite, aegirine-rich clinopyroxene, K-silicate phase) and a gas bubble.

In contrast to Ca-silicates, inclusions in zoned fluorapatite (5–50  $\mu\text{m}$ ) are rich in carbonate and other salt components and do not show silicate phases. They are oval or elongated in shape and localized in the central zones of the host mineral. The inclusions are usually fine-devitrified or completely crystallized and in places contain individual colorless phases such as nyerereite, calcite and halite (SEM-EDS, Fig. 4). No melt inclusions are found in the Sr-rich rim (up to 5 wt.% SrO) of zoned crystals, but it does contain rare crystallites of combeite.

## 6. Heating experiments with melt inclusions

About 100 heating experiments were performed on melt inclusions in phenocrysts (>75 – in nepheline, 20 – in apatite and 5 – in wollastonite). Clinopyroxene-hosted inclusions were not used for heating experiments because of poor visibility at high temperature.

### 6.1. Nepheline-hosted inclusions

These inclusions are very interesting because of their liquid immiscibility nature and phase behavior during heating. However, they are susceptible to leakage during heating experiments, especially at temperatures higher than 800–900  $^{\circ}\text{C}$ . The same problems were described by Bazarova et al. (1975) for nepheline-hosted inclusions in

nephelinites. They explained inclusion leakage as due to proposed structural inversion in host nepheline at  $T \approx 850$   $^{\circ}\text{C}$ . However, we were successful in obtaining the first homogenization (dissolution of a gas bubble in carbonate liquid) in some individual inclusions. However, complete homogenization (miscibility of the carbonate and silicate liquids) was not achieved with further temperature increase, even up to 1200  $^{\circ}\text{C}$ .

Heating experiments with glassy inclusions (glass + vapor-carbonate globule; glass + gas bubble + carbonate globule; glass + some vapor-carbonate globules  $\pm$  gas bubble) were mainly undertaken in the range 20–950  $^{\circ}\text{C}$ . First changes within inclusions were observed in the vapor-carbonate globule at 470–510  $^{\circ}\text{C}$  and interpreted to represent recrystallization of phases. The carbonate component of gas-carbonate globules melted instantaneously at 550–570  $^{\circ}\text{C}$ . Melting of silicate glass occurred at 600–670  $^{\circ}\text{C}$ . When some vapor-carbonate globules and gas bubbles were present in initial melt inclusions, they gradually moved in the silicate melt and commonly coalesced into one large vapor-carbonate bleb with increasing temperature. The appearance and then disappearance of small blebs of different salt liquids or new-formed phases (fluoride, chloride or sulfate) occurred in both silicate and carbonate melts between 670–840  $^{\circ}\text{C}$ . The salt and carbonate blebs then amalgamated again into one large globule, which gradually decreased in size and the gas bubble within it also decreased in size at 800–900  $^{\circ}\text{C}$ . The carbonate melt globule homogenized at 900–940  $^{\circ}\text{C}$  with the phase composition of these melt inclusions being silicate melt + carbonate liquid bleb. Quenching of such inclusions led to the initial phase

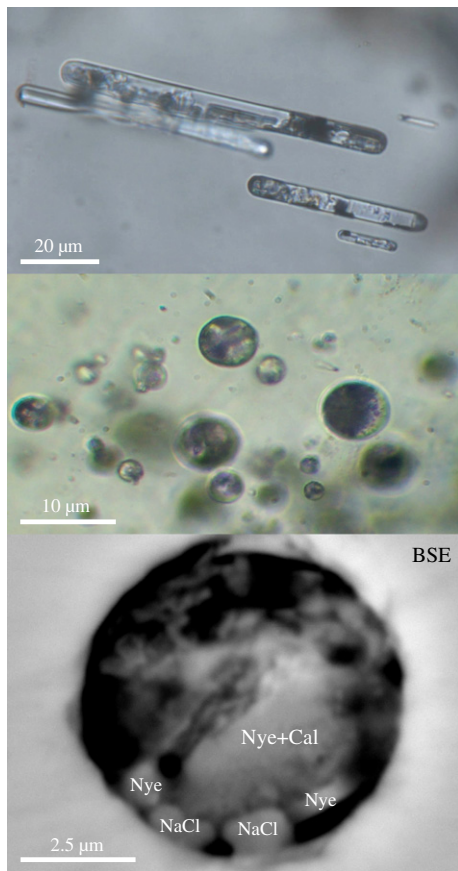


**Fig. 4.** Crystallized carbonate-salt melt inclusions in fluorapatite microphenocrysts, sample OI 7/2000, CWN, Oldoinyo Lengai. Symbols: Nye – nyerereite; Cal – calcite.

composition. The behavior of two nepheline-hosted individual inclusions during heating under different temperature regimes ( $\approx 50$  and  $100$  °C/min) is shown on Fig. 5.

Heating experiments with partly crystallized inclusions indicated the same relations for carbonate and silicate liquids and showed that the silicate daughter phases disappeared in silicate melt before homogenization in vapor-carbonate liquid globule ( $< 920$  °C). Transformation of daughter fluorite into the  $\text{CaF}_2$  liquid occurred at  $600$ – $630$  °C. Delhayelite, mica and then leucite disappeared into silicate melt in the temperature range  $670$ – $780$  °C. Clinopyroxene melted at  $890$ – $910$  °C.

## 6.2. Inclusions in fluorapatite and wollastonite

During heating experiments with carbonate-salt inclusions in fluorapatite the melting of colorless phases occurred at  $550$ – $720$  °C. They homogenized into carbonate-salt melt in the temperature range of  $900$ – $1130$  °C. The appearance and then disappearance of new-formed phases at  $990$ – $1090$  °C were observed in the inclusions with highest homogenization temperature ( $> 1100$  °C). Wollastonite-hosted inclusions homogenized into silicate melt at  $1085$ – $1130$  °C.

Previous thermometric data for a nephelinite from Oldoinyo Lengai has shown the following homogenization temperatures for mineral-hosted inclusions:  $1120$ – $1220$  °C – in nepheline and  $900$ – $1020$  °C – in wollastonite (Naumov et al., 1972).

## 7. Chemical composition of nepheline-hosted inclusions

### 7.1. Daughter phases

After preliminary optical and SEM identification of daughter phases in nepheline-hosted inclusions some of them (with

size  $> 5$  µm) have been analyzed by microprobe. Leucite, delhayelite, mica and fluorite are common daughter phases in partly crystallized inclusions, whereas clinopyroxene, wollastonite and K-feldspar occur rarely (Sharygin et al., 2009). Compositions of the daughter crystals from inclusions are given in Tables 2 and 3.

#### 7.1.1. Leucite

Colorless leucite from inclusions was previously labeled as an unidentified K–Al-silicate with leucitic composition (Sharygin et al., 2009). Petrographic observations of inclusions indicate prismatic habit of crystals (Fig. 3). It is known that high-temperature ( $> 1000$  °C) leucite is cubic phase and with decreasing of temperature ( $560$ – $715$  °C) it transforms into tetragonal polymorphs (Mazzi et al., 1976). Prismatic crystals, their melting at  $670$ – $780$  °C and leucitic composition strongly suggest that this leucite crystallized directly from silicate melt as a tetragonal phase. The mineral contains high  $\text{Fe}_2\text{O}_3$  (up to 9 wt.%), low  $\text{Al}_2\text{O}_3$  (15.3–17.5 wt.%) and appreciable  $\text{Na}_2\text{O}$  (0.1–0.5 wt.%), indicating a high abundance (up to 26 mol%) of the  $\text{KFeSi}_2\text{O}_6$  end-member (Table 2).

#### 7.1.2. Clinopyroxene and wollastonite

Daughter clinopyroxene is in places oscillatory-zoned (inclusion O8-1n2, Fig. 3). Its composition is characterized by moderate Mg number ( $\text{Mg}/(\text{Mg} + \text{Fe}^{2+}) - 0.4$ – $0.6$ ), low contents of  $\text{Al}_2\text{O}_3$  (0.4–1.0 wt.%),  $\text{TiO}_2$  (up to 1.4 wt.%) and  $\text{CaO}$  (13.0–19.0 wt.%) and appreciable amount of  $\text{Na}_2\text{O}$  (3.1–6.8 wt.%). In general, evolution of inclusion clinopyroxene trends towards aegirine-rich compositions, which is common in clinopyroxene phenocrysts and microphenocrysts in the Lengai CWNs (Dawson, 1998; Dawson and Hill, 1998; Klaudius and Keller, 2006). Wollastonite from the inclusions is close to ideal  $\text{Ca}_2\text{Si}_2\text{O}_7$  with minor  $\text{FeO}_t$  (0.8 wt.%) and  $\text{MnO}$  (0.4 wt.%) (Table 2).

#### 7.1.3. Tetraferriannite

Brown mica is an interstitial anhedron phase in partly crystallized inclusions in nepheline (Fig. 3). This phase is rich in  $\text{SiO}_2$ ,  $\text{FeO}_t$ ,  $\text{Na}_2\text{O}$ ,  $\text{TiO}_2$ , F and poor in  $\text{Al}_2\text{O}_3$  and  $\text{MgO}$  (Table 3). Calculations of formulae based on 11 oxygens show that this mica may contains water (up to 1.9 wt.%). This complex mica is characterized by equal abundances of end-members: annite, tetraferriannite, shirokshinite, and hypothetical Ti-rich compositions (Table 3). However, the predominance ( $> 50$  mol%) of the end-members with  $\text{Fe}^{2+}_3[\text{Fe}^{3+}\text{Si}_3\text{O}_{10}]$  proposes a classification of this mica as Na–Mg–Ti-rich tetraferriannite. The broad isomorphism between tainiolite  $\text{KMg}_2\text{Li}[\text{Si}_4\text{O}_{10}]\text{F}_2$  and shirokshinite  $\text{KMg}_2\text{Na}[\text{Si}_4\text{O}_{10}]\text{F}_2$  in peralkaline systems (Armbruster et al., 2007; Pekov et al., 2003) proposes the possible presence of Li in the Oldoinyo mica. Rb is not excluded as possible minor component. High contents of Li and Rb ( $> 200$  ppm) are detected by SIMS in residual peralkaline glasses of partly crystallized inclusions in nepheline phenocrysts (see Table 6).

#### 7.1.4. Delhayelite and fluorite

Colorless delhayelite forms sheaf-like aggregates in partly crystallized inclusions in nepheline (Fig. 3). The mineral from inclusions contains high concentrations of  $\text{Fe}_2\text{O}_3$ ,  $\text{TiO}_2$ ,  $\text{MgO}$  and S and low amounts of  $\text{Al}_2\text{O}_3$  (Table 3) supporting very specific composition of groundmass delhayelite previously reported in CWNs (Dawson, 1998; Dawson and Hill, 1998). These compositional features are remarkable in comparison with unaltered Khibiny delhayelite (Pekov et al., 2009 and references therein; Stoppa et al., 1997). It should be noted that delhayelite from nepheline-hosted inclusions are richer in F, S and poorer in Cl than that in the groundmass (Table 1). Like the groundmass mineral, some inclusion delhayelites are overgrown by a water-bearing phase which is poorer in alkalis, F, Cl and richer in  $\text{SiO}_2$  and  $\text{BaO}$  (hydrodelhayelite?). The high  $\text{Fe}_2\text{O}_3$  and low  $\text{Al}_2\text{O}_3$  strongly suggest that iron is incorporated into the tetrahedral site. The calculations on the basis of  $(\text{Si} + \text{Al} + \text{Fe}^{3+}) = 8$  indicate

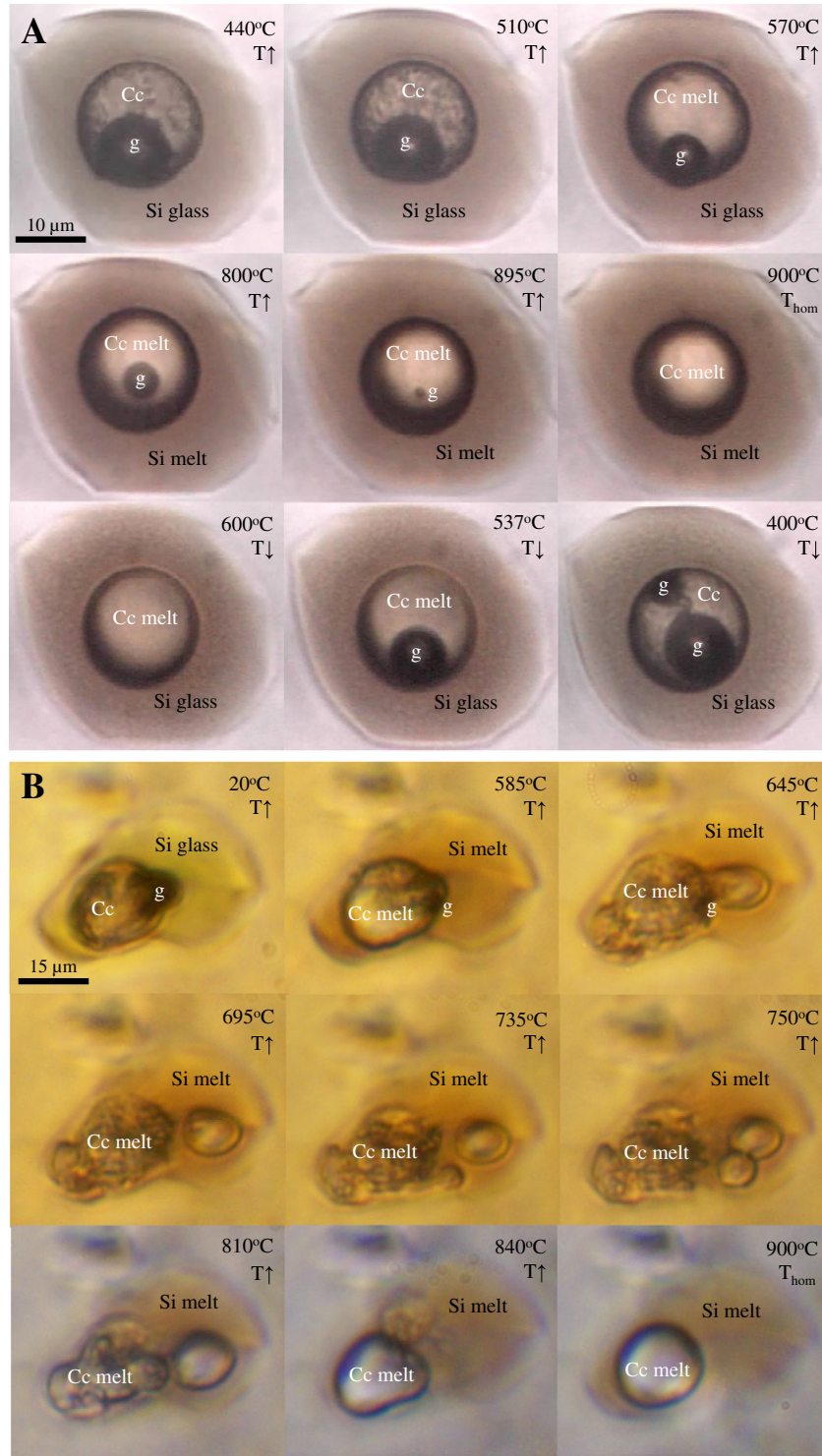


**Fig. 5.** Heating experiments with nepheline-hosted inclusions in different temperature regimes ( $A \approx 100$  °C/min;  $B \approx 50$  °C/min), sample Ol 7/2000, CWN, Oldoinyo Lengai. Symbols: Si glass – silicate nephelinite glass; Si melt – silicate nephelinite melt; Cc melt – natrocarbonatite melt. Other abbreviations (Cc, g) as in Fig. 2.

the formula for the Oldoinyo fresh delhayelite is close to  $K_4Na_2Ca_2[(Fe^{3+},Al)Si_7O_{19}]F_2Cl$ , where  $Fe^{3+}$  is up to 0.9 apfu. In general, this is  $Fe^{3+}$ -rich analog of delhayelite,  $K_4Na_2Ca_2[AlSi_7O_{19}]F_2Cl$  (Pekov et al., 2009). The incorporation of iron as  $Fe^{3+}$  in delhayelite is consistent with mineralogy of the Lengai CWNs, where the groundmass minerals contain high abundance of  $Fe_2O_3$  and some of them (nepheline, sodalite) may bear high  $Fe^{3+}$  in the tetrahedral

site (Dawson, 1998; Dawson and Hill, 1998; Kladius and Keller, 2006).

Daughter fluorite in silicate glass is close to ideal  $CaF_2$ , but contains appreciable Sr (up to 2.1 wt.%) and negligible Fe, Mg and Na (up to 0.1 wt.%, EMPA data). This phase is comparable in its Sr content with fluorite from fresh natrocarbonatites (0.5–3.9 wt.% Sr, Mitchell, 2006a; Zaitsev, 2010a).

**Table 2**  
Representative analyses (wt.%) of daughter Fe-rich leucite, clinopyroxene and wollastonite from nepheline-hosted inclusions, CWN, sample Ol 7/2000, Oldoinyo Lengai, Tanzania.

Mineral	Lc	Lc	Lc	Lc	Lc	Lc	Lc	Cpx			Cpx	Cpx	Wo
Inclusion number	09-1xn1	09-1xn2	09-1xn4	08-8n1	09-4n1	09-5n1	Ideal	08-1n2	08-1n2	08-1n2	09-17n5	08-1n5	09-14n3
n	11	7	1	1	1	2		2	2	2	1	1	2
								c	m	r			
wt.%													
SiO <sub>2</sub>	54.22	54.70	54.47	54.66	54.30	54.29	53.48	50.72	50.70	50.46	50.00	50.80	51.58
TiO <sub>2</sub>	0.08	0.06	0.19	0.00	0.03	0.05		1.36	1.21	1.01	1.00	1.36	0.00
ZrO <sub>2</sub>											0.28		
Al <sub>2</sub> O <sub>3</sub>	15.27	17.49	16.04	15.31	17.24	15.62	17.02	0.41	0.95	0.38	0.39	0.39	0.00
Fe <sub>2</sub> O <sub>3</sub> *	8.96	6.31	7.01	8.31	6.89	8.22	8.89	9.99	7.63	10.96	9.05	16.37	0.20
FeO*								11.53	8.93	9.87	12.15	6.73	0.69
MnO	0.12	0.08	0.16	0.07	0.04	0.07		0.76	0.53	0.72	0.69	0.72	0.43
MgO	0.21	0.08	0.12	0.14	0.16	0.14		4.36	7.74	4.99	5.15	3.42	0.12
CaO	0.09	0.05	0.09	0.16	0.02	0.03		15.20	18.95	16.41	16.43	13.03	46.84
Na <sub>2</sub> O	0.49	0.36	0.51	0.45	0.14	0.29	0.69	4.82	3.06	4.47	3.83	6.84	0.07
K <sub>2</sub> O	20.25	20.37	20.36	20.32	20.47	20.55	19.92						
Sum	99.69	99.50	98.95	99.42	99.29	99.26	100.00	99.15	99.70	99.27	98.97	99.66	99.93
<i>Formula</i>	<i>Based on 6 oxygens</i>						<i>Based on 4 cations and 6 oxygens</i>						
Si	2.039	2.037	2.050	2.055	2.031	2.046	2.000	1.986	1.947	1.970	1.968	1.970	2.000
Ti	0.002	0.002	0.005	0.000	0.001	0.001		0.040	0.035	0.030	0.030	0.040	0.000
Zr											0.005		
Al	0.677	0.768	0.712	0.678	0.760	0.694	0.750	0.019	0.043	0.017	0.018	0.018	0.000
Fe <sup>3+</sup>	0.253	0.177	0.199	0.235	0.194	0.233	0.250	0.294	0.221	0.322	0.268	0.478	0.006
Fe <sup>2+</sup>								0.378	0.287	0.322	0.400	0.218	0.022
Mn	0.004	0.003	0.005	0.002	0.001	0.002		0.025	0.017	0.024	0.023	0.024	0.014
Mg	0.012	0.004	0.007	0.008	0.009	0.008		0.254	0.443	0.290	0.302	0.198	0.007
Ca	0.004	0.002	0.004	0.006	0.001	0.001		0.638	0.780	0.687	0.693	0.541	1.946
Na	0.036	0.026	0.037	0.033	0.010	0.021	0.050	0.366	0.228	0.338	0.292	0.514	0.005
K	0.971	0.968	0.978	0.975	0.977	0.988	0.950						
Cation sum	3.997	3.986	3.996	3.992	3.984	3.994	4.000	4.000	4.000	4.000	4.000	4.000	4.000
Mg/(Mg + Fe <sup>2+</sup> )								0.40	0.61	0.47	0.43	0.48	
<i>End-members</i>													
CaAl <sub>2</sub> SiO <sub>6</sub>	0.3	0.2	0.4	0.6	0.1	0.1							
NaAlSi <sub>2</sub> O <sub>6</sub>	3.6	2.6	3.7	3.2	1.0	2.1	5.0						
KAlSi <sub>2</sub> O <sub>6</sub>	69.0	78.6	74.5	70.8	78.1	72.6	71.2						
KFeSi <sub>2</sub> O <sub>6</sub>	25.9	18.1	20.8	24.5	19.9	24.4	23.8						
KMg <sub>0.5</sub> Si <sub>2.5</sub> O <sub>6</sub>	1.2	0.4	0.7	0.8	0.9	0.8							

BaO, SrO, Nb<sub>2</sub>O<sub>5</sub>, P<sub>2</sub>O<sub>5</sub> are below detection limits.

Ideal composition for leucite is K<sub>0.95</sub>Na<sub>0.05</sub>Fe<sub>0.25</sub>Al<sub>0.75</sub>Si<sub>2</sub>O<sub>6</sub>. \* – Fe<sub>2</sub>O<sub>3</sub> and FeO for clinopyroxene and wollastonite are calculated from charge balance.

## 7.2. Glass

Silicate glass was analyzed by EMPA in more than 50 melt nepheline-hosted inclusions variable in phase composition from glassy to partly crystallized. Representative compositions of glass are given in Tables 4, 5 and 6.

### 7.2.1. Major elements

Compositional data show that the glasses are highly enriched in alkalis and peralkaline to ultraperalkaline ((Na + K)/Al = 2.5–9.5), and depleted in MgO (up to 1.5 wt.%). They are strongly variable in all major elements, especially in SiO<sub>2</sub> (43.6–53.0 wt.%), FeO<sub>t</sub> (6.0–17.0 wt.%), CaO (0.3–7.2 wt.%), Na<sub>2</sub>O + K<sub>2</sub>O (12.5–23.0 wt.%) and SO<sub>3</sub> + F + Cl (1.0–4.3 wt.%), depending on the phase composition of the inclusions (Fig. 6). For example, in partly crystallized inclusions with high abundance of Ca-rich daughter phases, the residual glass is depleted in CaO (<3 wt.%, Table 5). The most Si-undersaturated glass in partly crystallized inclusions approaches the groundmass glass (Table 1). In general, compositional variations for nepheline-hosted glasses from the 1917 eruption CWN (Fig. 6) are very similar to those from the recent Oldoinyo CWN ashes (2007–2008 eruptions) and the Nasira CWNs reported by Mitchell (2009) and Mitchell and Dawson (2012–this volume) with the exception of different K<sub>2</sub>O/Na<sub>2</sub>O ratios. The glasses analyzed by us are characterized by the pre-dominance of K<sub>2</sub>O over Na<sub>2</sub>O, whereas the previous data show the opposite.

### 7.2.2. Trace elements and H<sub>2</sub>O

Nine of the largest nepheline-hosted inclusions (>25 μm) with low amounts of daughter phases were selected for analysis of silicate glass by SIMS. These glasses are extremely poor in H<sub>2</sub>O (0.1–0.6 wt.%), Cr and Ta (<10 ppm) but rich in Ba (1720–6490), Sr (1880–6700), Zr (1440–2200), REE (520–1040), Nb (450–980), Rb (250–460), Pb (60–150) and Li (240–390 ppm) (Table 6). In contrast with glasses, the host nepheline contains only appreciable Rb (160 ppm), Sr (137 ppm), and Ba (35 ppm). Comparison of inclusion glasses and bulk IIB CWN show that the glasses are richer in incompatible and rare-earth elements; however their primitive mantle-normalized patterns (Fig. 7a) and chondrite-normalized diagrams (Fig. 7b) are very similar. In general, incompatible element ratios such as Th/U (1.5–2.2), Hf/Ta (1.8–3.1), Zr/Nb (1.6–2.6) and Ce/Pb (3.3–4.2) in glass are comparable with those in bulk CWN (1.1–3.6, 2–5, 2.6–4.8, 4.5–5.8, respectively) (Klaudius and Keller, 2006). Zr/Hf and Nb/Ta ratios dramatically increase from CWN to inclusion glass (50–80 vs. 82–124, 62.4 vs. 97.6–139.3) indicating the highly evolved character of the silicate glass. The contents of Li are higher in glass (240–390 ppm) than in bulk CWN (47–67 ppm) and are comparable to natrocarbonatite (211–294 ppm) (Halama et al., 2007).

### 7.3. Carbonate globule

The EDS and EMPA data show that the carbonate globules in nepheline-hosted silicate–melt inclusions are equivalent to

**Table 3**

Representative analyses (wt.%) of daughter Na–Mg–Ti-rich tetraferriannite and Fe-rich delhayelite from nepheline-hosted inclusions, CWN, sample OI 7/2000, Oldoinyo Lengai, Tanzania.

Mineral	Tfa	Tfa	Tfa	Dlh	Dlh	Dlh	Dlh	Dlh	Dlh
Inclusion number	09-1xn1	09-14n4	ideal	09-4n1	09-14n4	09-1xn1	09-1xn2	08-1n1	08-8n1
n	7	3		1	1	1	1	2	1
wt.%									
SiO <sub>2</sub>	39.75	41.89	39.97	46.95	45.68	45.73	45.07	44.87	45.00
TiO <sub>2</sub>	5.27	4.69	4.83	0.11	0.58	0.38	0.46	0.56	0.35
Al <sub>2</sub> O <sub>3</sub>	2.33	2.13	2.06	5.08	3.23	4.18	2.71	3.69	2.99
Fe <sub>2</sub> O <sub>3</sub> *	7.96	6.66	8.05	1.77	6.09	3.39	7.58	4.82	4.59
FeO*	25.12	22.62	26.07						
MnO	0.89	0.68		0.18	0.10	0.18	0.28	0.05	0.05
MgO	4.21	5.83	4.87	0.02	0.47	0.13	0.11	0.41	0.34
CaO	0.07	0.12		15.30	13.22	13.55	13.28	14.58	14.64
BaO	0.04	0.14		0.30	3.41	0.21	0.10	0.00	0.23
SrO		0.00		0.14	0.12				
Na <sub>2</sub> O	1.68	1.86	1.87	6.33	5.66	6.03	5.03	6.79	7.02
K <sub>2</sub> O	9.47	9.59	9.49	16.48	15.03	19.03	19.76	18.38	16.92
F	1.79	(2.28)	2.30			5.19	4.77	5.33	5.15
Cl	0.01	0.01		1.87	1.46	1.50	3.17	2.64	1.30
S	0.06	0.04		0.55	0.78	0.98	0.11	0.36	0.93
H <sub>2</sub> O*	1.87	1.86	1.46						
Sum	100.52	100.40	100.97	95.08	95.83	100.48	102.43	102.48	99.51
O = (F, Cl, S)	0.79	0.98	0.97	0.70	0.72	3.01	2.78	3.02	2.93
Sum	99.73	99.42	100.00	94.38	95.11	97.47	99.65	99.46	96.58
<i>Formula</i>	<i>Based on 11 oxygens</i>			<i>Based on (Si + Al + Fe<sup>2+</sup>) = 8</i>					
Si	3.280	3.391	3.300	6.921	6.759	6.876	6.681	6.793	6.926
Ti	0.327	0.285	0.300	0.012	0.065	0.043	0.051	0.064	0.040
Al	0.226	0.203	0.200	0.883	0.563	0.741	0.473	0.658	0.542
Fe <sup>3+</sup>	0.494	0.406	0.500	0.196	0.678	0.384	0.845	0.549	0.532
Fe <sup>2+</sup>	1.733	1.531	1.800						
Mn	0.062	0.046		0.022	0.012	0.023	0.036	0.007	0.006
Mg	0.517	0.703	0.600	0.005	0.105	0.030	0.025	0.091	0.077
Ca	0.007	0.010		2.417	2.096	2.183	2.109	2.364	2.414
Ba	0.001	0.005		0.017	0.198	0.012	0.006	0.000	0.014
Sr		0.000		0.012	0.010				
Na	0.269	0.292	0.300	1.809	1.624	1.758	1.446	1.993	2.095
K	0.997	0.991	1.000	3.099	2.837	3.650	3.737	3.550	3.322
Cation sum	7.913	7.864	8.000	15.393	14.946	15.698	15.409	16.069	15.969
F	0.468	(0.518)	0.600			2.468	2.236	2.550	2.507
OH	1.031	1.004	0.800						
O	0.494	0.406	0.600						
Cl	0.002	0.002		0.467	0.366	0.382	0.796	0.677	0.339
S	0.005	0.003		0.152	0.218	0.276	0.030	0.102	0.267
Mg/(Mg + Fe <sup>2+</sup> )	0.23	0.31	0.25						
<i>End-members</i>									
Na*	27.0	29.3	30.0						
Ti*	32.7	28.5	30.0						
Al*	22.6	20.3	20.0						
Fe*	17.7	21.9	20.0						

Nb<sub>2</sub>O<sub>5</sub>, ZrO<sub>2</sub>, P<sub>2</sub>O<sub>5</sub> are below detection limits.

Ideal composition for mica is K (Fe<sup>2+</sup><sub>1.8</sub>Mg<sub>0.6</sub>Ti<sub>0.3</sub>Na<sub>0.3</sub>) [Al<sub>0.2</sub>Fe<sup>3+</sup><sub>0.5</sub>Si<sub>3.3</sub>O<sub>10</sub>] (OH)<sub>0.8</sub>F<sub>0.6</sub>O<sub>0.6</sub>. \* – Fe<sub>2</sub>O<sub>3</sub>, FeO and H<sub>2</sub>O for mica are calculated from charge balance. Fe<sub>2</sub>O<sub>3</sub> is calculated only as tetrahedral Fe<sup>3+</sup>. Na\* – shirokshinite K (Mg, Fe)<sub>2</sub>Na [Si<sub>4</sub>O<sub>10</sub>] (F, OH)<sub>2</sub>, Ti\* – hypothetical KFe<sub>2</sub>Ti [Fe<sup>3+</sup>+Si<sub>3</sub>O<sub>10</sub>] O<sub>2</sub> and KFe<sub>2.5</sub>Ti<sub>0.5</sub> [Si<sub>4</sub>O<sub>10</sub>] O<sub>2</sub>, Al\* – annite K (Fe, Mg)<sub>3</sub> [AlSi<sub>3</sub>O<sub>10</sub>] (OH)<sub>2</sub>, Fe\* – tetraferriannite KFe<sub>3</sub> [Fe<sup>3+</sup>+Si<sub>3</sub>O<sub>10</sub>] (OH)<sub>2</sub>. Values in brackets are estimated as Na = 2 F in ideal shirokshinite KMg<sub>2</sub>Na [Si<sub>4</sub>O<sub>10</sub>] F<sub>2</sub>.

natrocarbonatite in composition with Na, Ca, K, Cl, F, S and P as major components (Mitchell, 2006a; Zaitsev, 2010a; Zaitsev et al., 2009). The SEM study of individual carbonate globules indicates the presence of calcite, nyerereite, Na-carbonate, fluorite, Ca–Mg–Fe-carbonate, halite, sylvite and alkali sulfates, and some may contain very high abundance of fluorite or carbonates (Fig. 8). Optical observations show that some globules are zoned suggesting enrichment of particular zones by one mineral. In most cases we were unable to fully quantify the bulk composition of individual carbonate globules in the studied inclusions mainly due to their rapid partial decomposition after exposure at the surface to form Na-water-bearing carbonate (trona?), apthitalite and Na–K-chlorides. This process strongly resembles degradation and alteration of the Oldoinyo natrocarbonatites, starting immediately after their eruption (Dawson, 1962; Genge et al., 2001; Mitchell, 2006b; Zaitsev, 2010a; Zaitsev and

Keller, 2006; Zaitsev et al., 2008). There was only a single case where we were successful in analyzing a globule by EMPA, but this composition does not reflect the bulk carbonate globule and is related to the outer zone enriched in fluorite (Table 4 and Fig. 8). Previously Mitchell (2009) was luckier in analyzing the coexisting silicate glass and carbonate globule in the nepheline-hosted inclusions. However, these compositional data for bulk carbonate globule show very broad variations in CaO, Na<sub>2</sub>O + K<sub>2</sub>O, SO<sub>3</sub> and Cl despite approximately constant composition of silicate glass. Those compositional variations also seem to be related to inhomogeneity within a carbonate globule.

Seventeen LA-ICP-MS analyses have been obtained for non-opened carbonate globules from individual silicate–melt inclusions in nepheline. However, we were unable to correctly quantify the trace element composition of the carbonate globule because the

**Table 4**  
Chemical composition (wt.%) of silicate glasses and carbonatite globule in immiscible melt inclusions in nepheline phenocrysts, CWN, sample Ol 7/2000, Oldoinyo Lengai, Tanzania.

Inc.number	09-4n2	09-5n2	09-7n1	09-8n1	09-9n1	09-14n1	09-17n4	09-18n1	08-12n1	08-14n2	08-16n1	08-18n2	09-1xn3	09-1xn3
Phase	Gl	Gl	Gl	Gl	Gl	Gl	Gl	Gl	Gl	Gl	Gl	Gl	Gl	Cc
n	2	2	2	1	6	2	1	1	2	1	1	1	1	2
wt.%														
SiO <sub>2</sub>	50.65	51.91	45.62	47.85	51.11	50.47	47.45	53.29	52.04	47.66	46.63	53.02	48.93	3.10
TiO <sub>2</sub>	1.49	1.03	2.53	2.44	1.55	1.59	3.36	0.72	1.45	1.25	1.51	1.36	2.97	0.18
ZrO <sub>2</sub>	0.17	0.17	0.08	0.19	0.16	0.16	0.11	0.00						
Al <sub>2</sub> O <sub>3</sub>	3.99	5.69	2.66	9.13	4.81	4.69	2.20	4.43	5.60	6.64	5.10	4.51	3.23	1.13
FeO	13.71	10.05	16.85	9.94	11.42	11.45	16.86	11.90	10.67	13.56	7.54	10.52	12.30	0.72
MnO	0.77	0.51	0.87	0.54	0.60	0.57	0.86	0.52	0.64	0.63	0.46	0.49	0.83	0.07
MgO	0.73	0.52	0.91	0.62	0.55	0.59	0.88	0.69	0.65	1.33	0.60	0.75	0.62	0.28
CaO	3.95	5.31	1.59	7.62	4.58	5.48	5.01	5.55	4.44	5.39	10.26	5.95	5.83	37.02
BaO	0.49	0.16	2.50	0.33	0.20	0.11	0.32	0.36	0.37	0.31	0.33	0.30	0.04	0.38
SrO	0.32	0.09	0.44	0.15	0.09	0.08	0.37	0.14						
Na <sub>2</sub> O	6.06	7.53	7.56	5.42	8.87	6.96	6.42	5.69	7.66	8.14	10.65	6.54	5.13	3.41
K <sub>2</sub> O	10.58	10.62	10.03	11.54	9.92	10.52	9.36	9.18	11.90	10.20	9.02	10.52	9.49	2.08
P <sub>2</sub> O <sub>5</sub>	0.12	0.09	0.43	0.15	0.11	0.08	0.28	0.15	0.11	0.25	0.21	0.20	0.29	5.24
F									0.92	1.16	2.29	1.26	1.04	18.04
Cl	0.38	0.26	0.69	0.27	0.30	0.25	0.15	0.25	0.26	0.47	0.21	0.30	0.27	0.31
SO <sub>3</sub>	0.96	0.60	3.09	0.90	1.22	0.91	2.80	0.65	1.19	1.38	0.82	1.39	1.24	2.22
Total	94.37	94.54	95.85	97.09	95.49	93.91	96.43	93.52	97.90	98.37	95.63	97.11	92.21	74.18
O = (F, Cl) <sub>2</sub>	0.09	0.06	0.16	0.06	0.07	0.06	0.03	0.06	0.45	0.59	1.01	0.60	0.50	7.66
Total	94.28	94.48	95.69	97.03	95.42	93.85	96.40	93.46	97.45	97.78	94.62	96.51	91.71	66.52
(Na + K)/Al	5.38	4.20	8.77	2.34	5.27	4.87	9.41	4.36	4.55	3.68	5.35	4.91	5.79	

major composition or content of particular element in globule was unknown. As an example the LA-ICP-MS spectrum for a carbonate globule from a carbonate-rich inclusion is shown on Fig. 9. This spectrum indicates high abundance of most trace elements in the globule with respect to the host nepheline and also shows approximately equal contents of Rb and Cs in both globule and host mineral. The content of Rb in CWN nepheline is 160 ppm (SIMS, Table 6) and in fresh natrocarbonatites is 130–285 ppm (Simonetti et al., 1997; Zaitsev, 2010a; Zaitsev et al., 2008, 2009).

## 8. Discussion

### 8.1. Evolution of Oldoinyo Lengai

Several types of peralkaline magmas are involved in the evolution of Oldoinyo Lengai: olivine melilitite, phonolite, nephelinite and

natrocarbonatite (Donaldson et al., 1987; Keller et al., 2006; Klaudius and Keller, 2006). A liquid immiscibility relationship has been suggested between peralkaline silicic rocks and natrocarbonatite at Lengai based on volcanological, geochemical and isotopic data (Bell and Dawson, 1995; Church and Jones, 1995; Dawson, 1989, 1998; Dawson et al., 1996; Halama et al., 2007; Keller and Spettel, 1995; Keller et al., 2010; Mitchell, 2009; Peterson, 1989a, b, 1990; Simonetti et al., 1997; Williams et al., 1986). Numerous experiments simulating the Lengai natrocarbonatite and related silicate compositions also support immiscibility (Brooker and Kjarsgaard, 2011; Cooper et al., 1975; Hamilton et al., 1979; Jago, 1991; Jago and Gittins, 1991; Kjarsgaard and Peterson, 1991; Kjarsgaard et al., 1995; Lee and Wyllie, 1994, 1998; Mitchell and Kjarsgaard, 2008, 2011; Veksler et al., 2012). Petrographic evidence of coexistence of silicate and carbonatite melts has been observed in the Oldoinyo Lengai rocks intermediate between silicate rocks and natrocarbonatites

**Table 5**  
Chemical composition (wt.%) of residual glasses in partly crystallized melt inclusions in nepheline phenocrysts, CWN, sample Ol 7/2000, Oldoinyo Lengai, Tanzania.

Inc. number	09-5n1	09-14n3	09-14n4	08-1n1	08-8n1	09-1xn1	09-1xn2	09-3xn2	09-1xn4	08-1n5
n	1	3	3	3	2	2	2	2	1	1
Daughter phases	Lc, Tfa	Wo, Dlh	Flu, Tfa, Dlh, Lc	Flu, Delh	Flu, Lc, Dlh	Lc, Wo, Tfa, Dlh, Flu	Lc, Tfa, Dlh	Dlh, Flu	Lc	Cpx
wt.%										
SiO <sub>2</sub>	50.85	51.66	52.81	45.51	51.52	53.43	47.98	49.73	51.19	52.70
TiO <sub>2</sub>	0.42	1.18	2.51	1.40	1.98	2.08	2.21	2.32	1.59	1.56
ZrO <sub>2</sub>	0.21	0.11	0.25							
Al <sub>2</sub> O <sub>3</sub>	9.59	6.20	3.38		3.44	3.02	4.43	3.31	2.87	6.23
FeO	12.63	11.79	13.98	16.64	15.41	15.30	12.68	16.32	10.47	6.25
MnO	0.73	0.54	0.98	0.79	1.19	1.28	1.55	0.93	0.78	0.61
MgO	0.05	0.43	0.28	1.50	0.64	0.19	0.23	0.72	0.38	0.37
CaO	0.74	1.63	0.40	1.75	1.52	0.32	3.76	1.64	6.08	6.19
BaO	0.23	0.25	0.46	0.47	0.36	0.25	0.46	0.11	0.14	0.25
SrO	0.03	0.06	0.22							
Na <sub>2</sub> O	5.19	7.16	5.13	6.26	7.40	4.64	8.72	7.83	5.85	9.52
K <sub>2</sub> O	14.23	11.37	11.14	16.46	10.70	7.79	10.47	9.26	8.89	12.84
P <sub>2</sub> O <sub>5</sub>	0.03	0.06	0.06	0.19	0.15	0.15	0.08	0.21	0.14	0.19
F				0.63	0.67	0.62	0.92	1.30	1.18	1.22
Cl	0.27	0.15	0.07	0.03	0.01	0.02	0.06	0.11	0.43	0.21
SO <sub>3</sub>	0.70	0.67	1.19	1.26	0.85	1.60	1.52	1.13	0.92	0.57
Total	95.90	93.26	92.86	96.33	95.42	90.39	95.07	94.92	90.91	98.71
O = (F, Cl) <sub>2</sub>	0.06	0.03	0.02	0.27	0.28	0.27	0.40	0.57	0.59	0.56
Total	95.84	93.23	92.84	96.06	95.14	90.12	94.67	94.35	90.32	98.15
(Na + K)/Al	2.50	3.88	6.06	8.18	7.87	5.92	5.80	6.92	6.71	4.74

Table 6

Major and trace element composition for host rocks, nepheline phenocryst and silicate glasses of large nepheline-hosted inclusions, CWN, Oldoinyo Lengai volcano.

Wt.%	Rocks		Ne	Glasses of inclusions in nepheline								
	OL7	OL788	OL7-Ne	08-13n1	08-13n2	08-13n3	08-9n1	08-1n2	08-1n3	08-1n4	08-3n2	08-3n1
SiO <sub>2</sub>	43.50	44.58	43.15	50.66	50.93	50.85	50.31	50.84	52.36	52.32	52.87	51.02
TiO <sub>2</sub>	0.95	1.06	0.00	1.81	1.11	2.02	1.38	1.50	1.25	1.10	1.34	1.55
Al <sub>2</sub> O <sub>3</sub>	13.89	13.51	32.76	3.24	4.93	4.74	3.43	4.94	5.43	4.15	5.26	4.42
FeO	7.86	8.79	0.82	13.65	9.67	9.01	10.69	10.20	9.57	10.67	10.22	11.20
MnO	0.33	0.35	0.00	0.74	0.50	0.51	0.58	0.61	0.45	0.52	0.49	0.56
MgO	0.90	0.93	0.00	1.24	0.55	0.24	0.87	0.61	0.60	0.69	0.64	0.71
CaO	10.97	7.44	0.05	3.89	5.16	5.60	6.77	4.99	5.39	6.25	4.74	5.62
Na <sub>2</sub> O	12.00	12.71	15.21	7.46	8.47	7.61	8.38	8.84	9.34	7.38	7.63	7.18
K <sub>2</sub> O	4.87	5.42	8.42	9.61	11.42	11.48	9.75	11.13	12.06	10.87	11.14	11.42
P <sub>2</sub> O <sub>5</sub>	0.65	0.42	0.00	0.20	0.10	0.09	0.19	0.16	0.15	0.16	0.11	0.13
F	0.38		0.00	0.98	1.21	1.11	2.02	1.53	1.18	1.20	0.86	1.10
Cl			0.00	0.32	0.24	0.32	0.27	0.25	0.25	0.29	0.24	0.27
SO <sub>3</sub>	0.31		0.00	1.27	0.92	0.72	1.27	1.68	0.95	1.14	0.91	1.10
H <sub>2</sub> O	1.10			0.62	0.46	0.32	0.28		0.14		0.55	0.33
CO <sub>2</sub>	1.30											
LOI		1.66										
Total	99.01	96.87	100.41	95.69	95.67	94.62	96.19	97.28	99.12	96.74	97.00	96.61
O = (F, Cl) <sub>2</sub>	0.16		0.00	0.48	0.56	0.54	0.91	0.70	0.55	0.57	0.42	0.52
Total	98.85	96.87	100.41	95.20	95.11	94.08	95.27	96.58	98.56	96.17	96.59	96.09
PI	1.80	1.98	1.04	7.00	5.33	5.26	7.10	5.38	5.23	5.76	4.68	5.47
<i>ppm</i>												
La	145	148	0.23	308	219	133	298	328	186	195	230	281
Ce		209	0.23	504	368	254	485	535	327	355	385	456
Pr		19.2										
Nd		60	0.15	147	108	74	142	152	93	98	122	143
Sm		8.7	0.07	23	16	15	21	21	15	17	18	22
Eu		2.6	0.01	12.4	4.1	3.6	7.3	7.0	4.8	5.5	5.9	5.0
Gd		6.9	0.01	24	20	21	30	26	24	17	24	25
Tb		0.92										
Dy		4.78	0.00	12.2	7.9	9.1	13.2	11.5	7.8	8.2	10.7	12.3
Ho		0.83										
Er		2.3	0.01	5.6	4.4	5.4	7.0	6.8	4.9	5.1	5.9	7.4
Tm		0.34										
Yb		2.2	0.02	3.7	1.1	1.8	2.9	2.4	1.1	3.3	3.2	3.3
Lu		0.35	0.01	1.4	0.71	0.75	1.0		0.78	0.87	1.0	1.1
Sum REE		466.12	0.73	1041.30	749.21	517.65	1007.40	1089.70	664.38	704.97	805.70	956.10
Y	46	29	0.10	67	39	40	64	57	41	44	58	63
Zr	800	843	0.45	2019	1908	1146	2212	1451	1436	1533	1862	1535
Hf	12.4	10.63	0.01	21	20	14	20	14	13	16	15	15
Nb	295	299	0.59	939	795	444	877	761	591	612	856	975
Ta	5.0	4.92	0.01	7.2	6.5	4.5	6.6	7.8	4.8	5.3	7.1	7.0
Cr	10	5	1.15	4.8	5.9	4.0	10	8.8	6.4	6.4	7.3	11
V	215	184	18.8	265	209	136	267	253	170	176	223	260
Cu		43	1.75	328	218	205	427	287	205	208	245	271
Th	18	14.8	0.03	37	42	20	42	30	33	33	40	37
U	9	7.8	0.02	21	19	11	23	15	17	18	22	25
Pb		41	1.16	155	91	60	124	134	83	87	115	128
Ba	1560	1970	35.2	6485	1823	1715	3080	2585	1892	3045	2510	2096
Sr	2325	2167	137	6696	2012	1987	3733	2532	2283		2237	1881
Rb	110	110	160	400	272	270	401	456	253		361	318
Cs			0.28	12.5	5.4	5.9	7.4		6.0		8.4	13.7
Li			3.1	387	279	243	461		245		268	239
B			0.46	50	33	25	47		29		44	31
Be		14.4	3.9	37	29	19	37		36		33	26

Data for rocks are from Keller and Krafft (1990), Keller and Spettel (1995), Klaudius and Keller (2006). Composition of nepheline and inclusion glasses were analyzed by EMPA (major elements) and SIMS (trace elements, H<sub>2</sub>O). Ne – nepheline phenocryst containing silicate melt inclusions.

and in the Nasira CWNs (Church and Jones, 1995; Dawson et al., 1996; Mitchell and Dawson, 2012–this volume).

However, all previous data fail to document the compositions of pre-immiscible primary melt and co-magmatic silicate–carbonatite liquids, and the timing and conditions of separation of these two melts. Olivine melilitite and olivine nephelinite have been proposed as parental melts for the evolution of the Lengai suite (Dawson, 1998; Keller et al., 2006; Peterson and Kjarsgaard, 1995). However, more Si-saturated compositions (phonolites, CWNs) and natrocarbonatites cannot be derived by ordinary crystal fractionation

from olivine melilitite (Klaudius and Keller, 2006). Additional processes (assimilation of country rocks, mixing of different mantle components, liquid immiscibility, fluid exsolution, etc.) strongly need to be involved (Dawson, 1998; Keller et al., 2006; Klaudius and Keller, 2006).

In this context the study of melt inclusions trapped by minerals can give more information about relationships of coexisting peralkaline silicate and natrocarbonatite melts as well as their compositions and PT-conditions, than a study of the bulk composition and mineralogy for separate rocks.

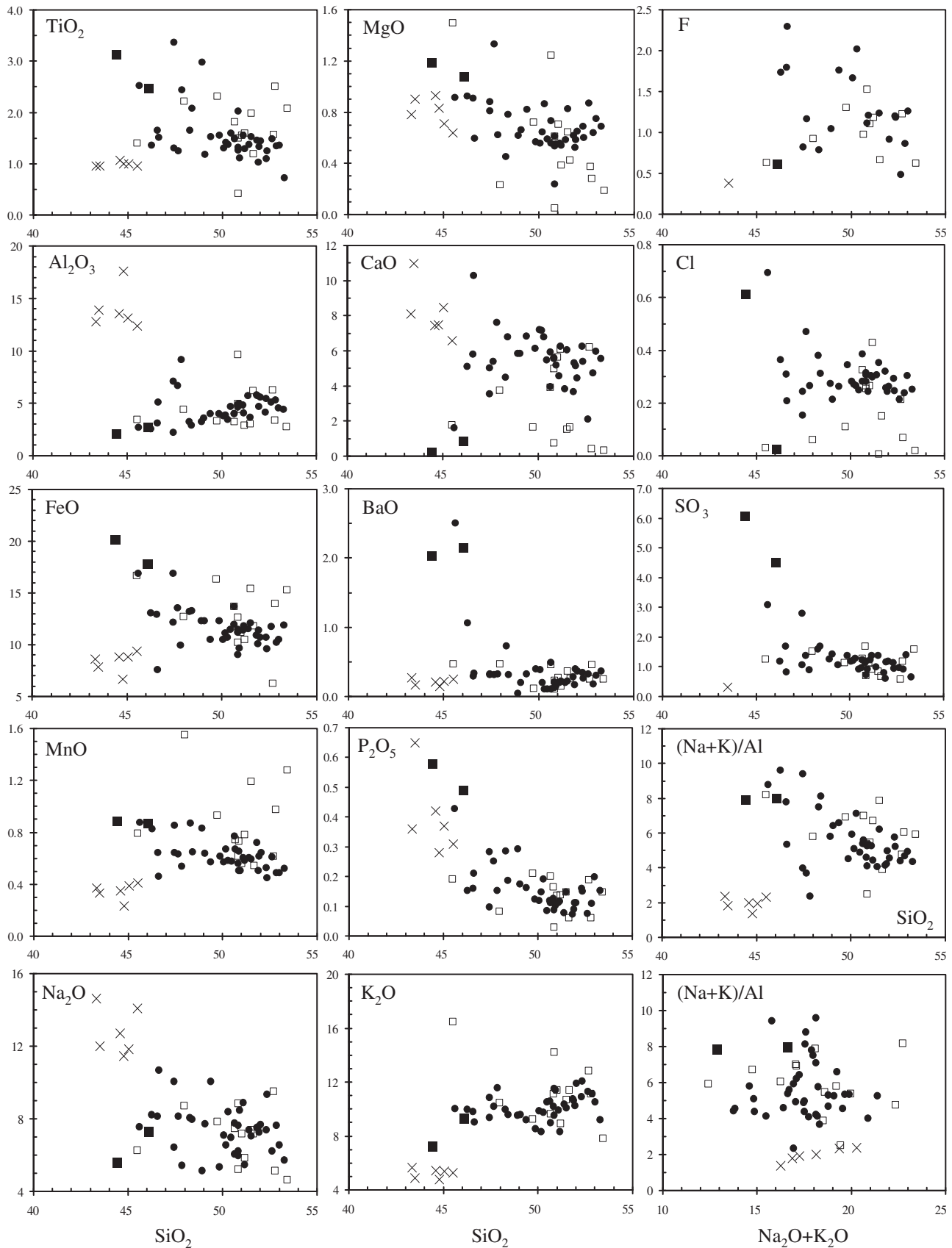


**Fig. 6.** Compositional variations for silicate glasses of nepheline-hosted inclusions, groundmass glasses (sample OI 7/2000, CWN) and CWN IIB rocks, Oldoinyo Lengai volcano. Symbols: crosses – combeite wollastonite nephelinites CWN IIB (Keller and Krafft, 1990; Keller and Spettel, 1995; Klaudius and Keller, 2006); filled circles – glasses of melt inclusions in nepheline phenocrysts with following compositions: glass + vapor-carbonate globule and glass + gas  $\pm$  trapped phases; open squares – glasses of partly crystallized inclusions in nepheline (glass + daughter phases + gas); filled squares – groundmass glasses.

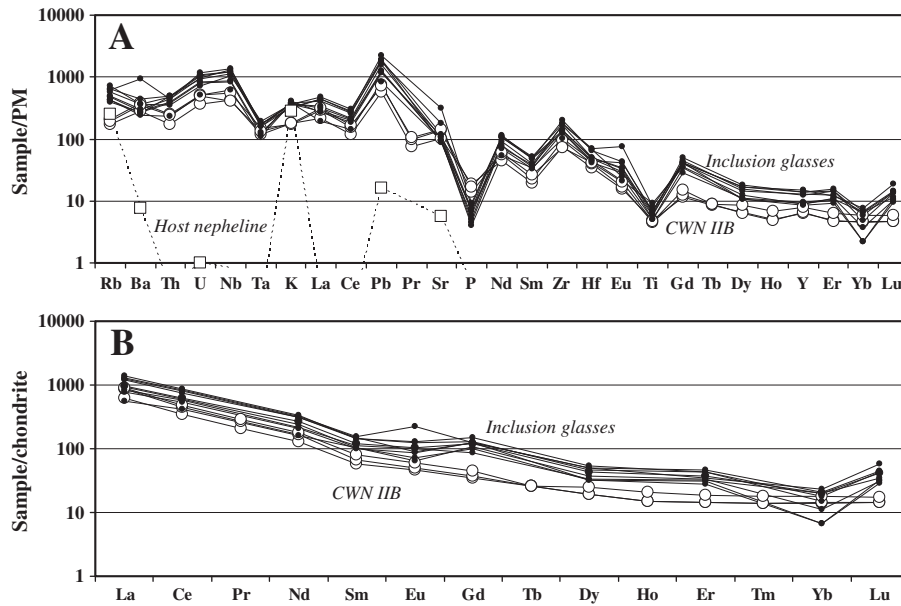


**Fig. 7.** (A) Primitive mantle-normalized incompatible trace element abundances in Oldoinyo Lengai IIB combeite wollastonite nephelinites (CWN IIB) and glasses of nepheline-hosted inclusions from sample OI 7/2000, CWN. (B) Chondrite-normalized REE diagram. Normalizing values are from McDonough and Sun (1995). Samples OL788, OL804 and OL230 from Klaudius and Keller (2006) are used as reference CWN IIB rocks.

8.2. Nephelinite–natrocarbonatite liquid immiscibility in melt inclusions

Recent reports (Mitchell, 2009; Mitchell and Dawson, 2012-this volume) and our melt inclusion data clearly show that silicate–carbonate immiscibility is a very common phenomenon at Oldoinyo Lengai, which is evident both at the macroscale (volcanic eruptions) and at the microscale (inclusions in minerals). Nepheline-hosted inclusions in the 1917 CWN lavas show a very complicated history during cooling of initial silicate melt as suggested by Dawson (1998). The occurrence of melt inclusions in phenocrysts and some microphenocrysts strongly suggests that their formation began in a near-surface intermediate chamber. According to our heating experiments with the 1917 CWN the silicate–natrocarbonatite immiscibility took place

at temperatures higher than 1130 °C. Moreover, nepheline and fluorapatite phenocrysts crystallized in an intermediate chamber when initial carbonated silicate melt was not homogeneous and represented a mixture of two or three immiscible liquids (peralkaline silicate, natrocarbonatite, and sulfide). This is supported by the coexistence of silicate–melt inclusions with various ratios of carbonate + gas to silicate glass in the nepheline cores (Fig. 1), the presence of individual sulfide inclusions in nepheline and carbonate–salt inclusions in fluorapatite (Fig. 4). Consequently, the initial silicate melt for our CWN lava flow might not be a pure silicate product of complete silicate–natrocarbonatite immiscibility in an intermediate chamber, but may represent an intermediate composition (silicate melt + small amount of natrocarbonatite liquid blebs). In addition, on the basis of silicate–carbonate relations in CWNs and their mineral-hosted inclusions Mitchell and Dawson (2012-this volume) assumed that none of the bulk compositions of CWN II lavas at Oldoinyo Lengai are considered to represent those of parental liquids as their compositions reflect rheological (phenocryst accumulation, cumulate disruption) and assimilation processes. In general, the behavior of natrocarbonatite bleb and its relationship to a gas phase during the heating of nepheline-hosted silicate–melt inclusions clearly show that the separated natrocarbonatite was undoubtedly a carbonate melt, rather than a cognate fluid condensate as suggested by Nielsen and Veksler (2002).

Surprisingly, a preliminary study for an ijolite xenolith from Oldoinyo Lengai has indicated very low abundance of carbonate (<10 vol.%) in nepheline-hosted silicate–melt inclusions (Sharygin et al., 2010). Ijolites and other plutonic xenoliths at Oldoinyo Lengai are considered as cumulate rocks formed in a sub-volcanic magma chamber (Dawson et al., 1995a, 1995b). The low carbonate content and predominance of a gas phase over carbonate in the inclusions in our ijolite possibly suggest that crystallization of these rocks occurred beyond of the limits of silicate–carbonate immiscibility.

Further scenarios for natrocarbonatite melts both trapped by minerals as inclusions and occurring as blebs in host silicate magma probably were quite different. Homogenization in the carbonate globule (dissolution of gas bubble in carbonate melt) at 900–940 °C assumes that after separation from silicate magma the natrocarbonatite represented a homogeneous liquid in the 900–1130 °C temperature range. Within inclusions (closed system) the fluid phase and salt–carbonate

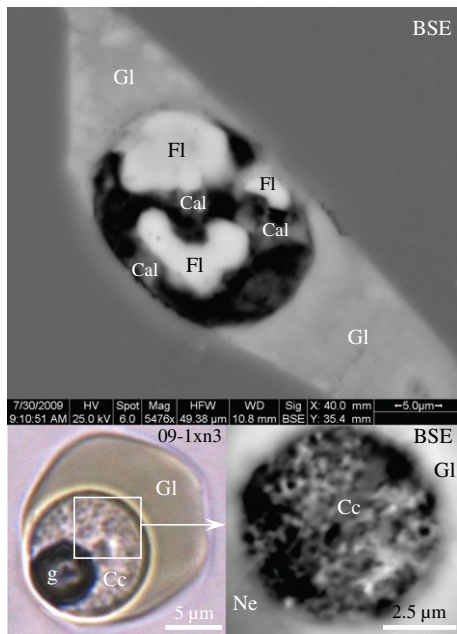


**Fig. 8.** Natrocarbonatite globules in nepheline-hosted silicate–melt inclusions, sample OI 7/2000, CWN. Chemical data for the inclusion 09-1xn3 see Table 4. Symbols see Figs. 2 and 4.

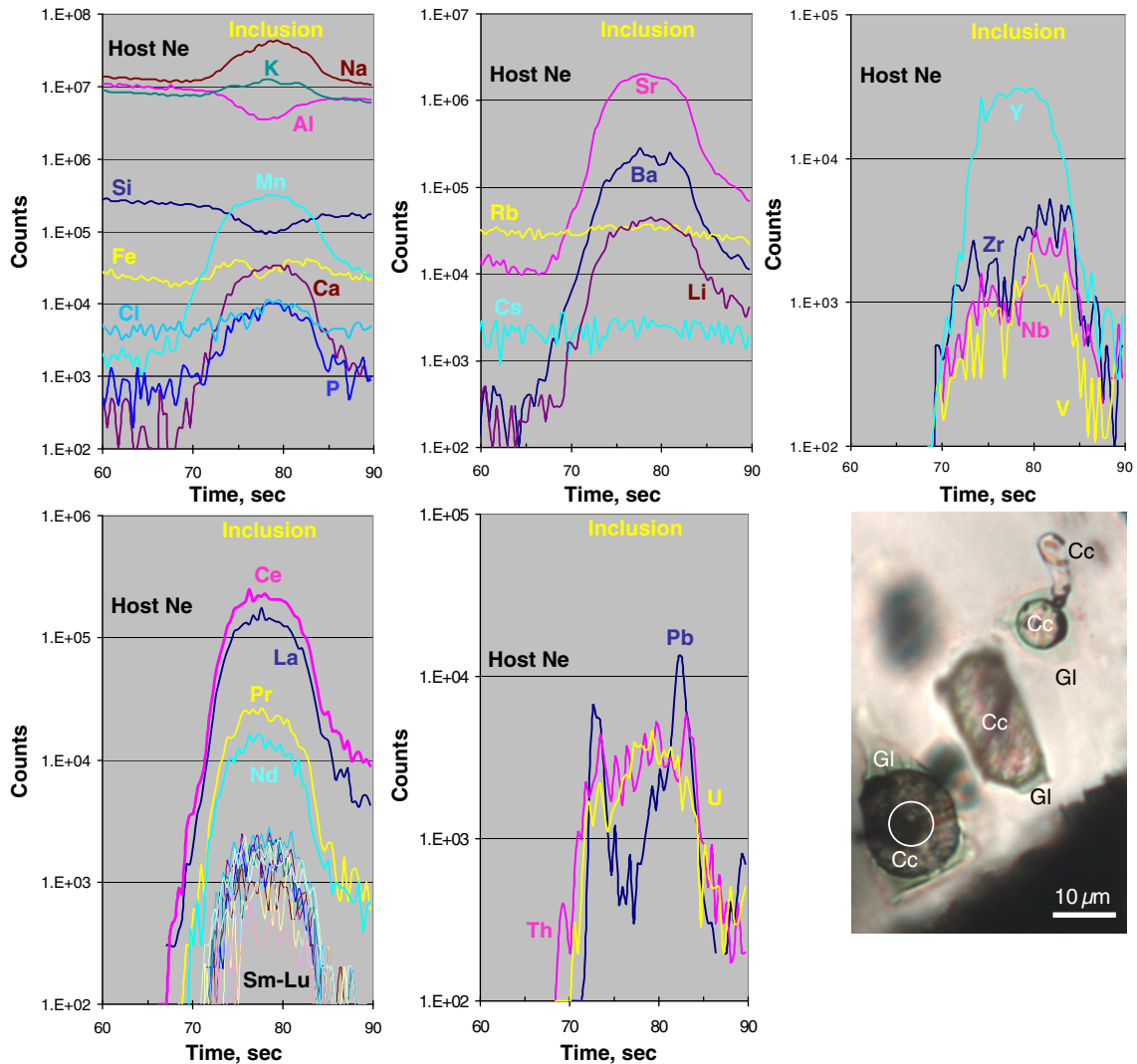


**Fig. 9.** LA-ICP-MS spectrum for a natrocarbonatite-rich melt inclusion in the core of nepheline phenocryst, sample Ol 7/2000, CWN, Oldoinyo Lengai. White circle on the photo means analyzed part of the inclusion.

liquids of different compositions (carbonate, fluoride, chloride, and sulfate) may have separated from natrocarbonatite melt in the 900–600 °C range until quenching of the silicate melt into glass. The presence of nepheline-hosted melt inclusions with numerous individual carbonate globules possibly supports this idea (Figs. 1 and 2), as these individual globules may have different compositions. Multi-stage liquid immiscibility has been proposed for mineral-hosted inclusions from the Krestovskii massif, Polar Siberia (Panina, 2005). Carbonate–carbonate immiscibility (Mitchell, 1997) and reaction between carbonate and silicate liquids (Mitchell and Dawson, 2012–this volume) cannot be excluded. However, if most of these immiscible liquids are metastable and ephemeral, the separation of a  $\text{CaF}_2$ -rich fluoride melt is more realistic. This is supported by the presence of daughter fluorite in partly crystallized inclusions in nepheline. Rare inclusions in nepheline may contain individual gas bubble, carbonate homogeneous globule and octahedral crystal of fluorite in silicate glass. During heating this fluorite transformed into a fluoride melt rather than dissolving in silicate melt at temperature higher than 600 °C. Further increase of temperature led to coalescing of this melt with the existing vapor-carbonate bleb.  $\text{CaF}_2$ -silicate liquid immiscibility is also observed in nepheline-hosted inclusions from the Sadiman and Mosonik nephelinites within the Gregory Rift (Zaitsev et al., 2012–this volume; unpublished data of V.V. Sharygin).

Unlike the behavior documented in the inclusions, during complete crystallization of CWN lavas (open system) the silicate–natrocarbonatite immiscibility was commonly obscured due to degassing of the silicate melt, disappearance of carbonate liquid into silicate melt and/or reaction of carbonate melt with early silicate minerals. The existence of a combeite corona around wollastonite in CWNs seems to be a result of reaction between natrocarbonatite and silicate. Moreover, Mitchell and Dawson (2012–this volume) have indicated that namely assimilation of natrocarbonatite melt, which is previously exsolved in the magma chamber(s) underlying Oldoinyo Lengai, led to the formation of combeite in CWNs. The individual natrocarbonatite blebs are preserved only in quenched CWN types containing a high abundance of groundmass silicate glass (Mitchell and Dawson, 2012–this volume).

### 8.3. Initial composition of immiscible natrocarbonatite melt

The ubiquitous presence of nyerereite, calcite and fluorite in gas-carbonate globules of nepheline-hosted inclusions in our CWN suggests that initial immiscible natrocarbonatite is closely related to the carbonate-rich part of the system  $\text{Na}_2\text{CO}_3$ – $\text{CaCO}_3$ – $\text{CaF}_2$ . Unfortunately, the previous chemical data for carbonate globules in nepheline-hosted inclusions from the 2007–2008 Lengai eruptions

(Mitchell, 2009) did not give the fluorine content. In general, fluorine has a great influence on phase equilibria involving both natrocarbonatite and calcicarbonatite compositions. For example, the presence of 8 wt.% F in the system  $\text{Na}_2\text{CO}_3\text{--CaCO}_3$  reduces the minimum melting temperatures of phases and liquidus temperature to  $\sim 200^\circ\text{C}$  for compositions with 50%  $\text{Na}_2\text{CO}_3$  and 50%  $\text{CaCO}_3$  (Jago, 1991; Jago and Gittins, 1991).

As mentioned above, we suggest the possibility of multistage immiscibility of initial natrocarbonatite melt which previously separated from silicate liquid. However, in the case of the presence of only one vapor-carbonate globule in the glassy inclusions we have to assume that its composition probably reflects the initial immiscible natrocarbonatite melt. Our heating experiments with those inclusions (Fig. 5a) have shown that the carbonate component of a vapor-carbonate globule transformed instantaneously into carbonate melt at  $550\text{--}570^\circ\text{C}$ . Such behavior seems to be related to the process occurring on the  $558\text{--}578^\circ\text{C}$  eutectic line in the  $\text{Na}_2\text{CO}_3\text{--CaCO}_3\text{--CaF}_2$  phase diagram (Jago, 1991; Jago and Gittins, 1991). Thus, bulk natrocarbonatite melt may be estimated as  $\approx 20\%$   $\text{CaF}_2$ ,  $40\text{--}60\%$   $\text{Na}_2\text{CO}_3$  ( $\pm \text{K}_2\text{CO}_3$ ) and  $20\text{--}40\%$   $\text{CaCO}_3$ . Of course, this bulk composition is highly simplified because it does not reflect the presence of other important components such as K, P, S and Cl that occur in natural natrocarbonatites, and we cannot estimate the degree of exchange by mobile elements between early minerals, silicate and carbonate liquids. However, such F-rich natrocarbonatite species enriched in fluorite and neighborite are observed among recent eruption products at Lengai (Keller and Krafft, 1990; Mitchell, 1997, 2006a, 2006b; Zaitsev, 2010a).

#### 8.4. Evolution of immiscible peralkaline silicate melt

Mitchell and Dawson (2012-this volume) have proposed that the size of the liquid immiscibility field for carbonated nephelinitic magmas is a function of their peralkalinity and have shown two trends for the CWN groundmass glasses. Our compositional data for immiscible melt inclusions in the 1917 eruption CWN indicate that silicate glasses have a high peralkaline index ( $(\text{Na} + \text{K})/\text{Al}$  – up to 9.5) that seems to be a signature inherited from the pre-immiscible magma. In terms of major and trace elements the inclusion glasses represent the most evolved compositions with Zr/Hf and Nb/Ta ratios and Li contents which are very much higher than in the host CWN. It should be noted that the immiscible nephelinite melt was virtually free of water ( $\text{H}_2\text{O}$  – up to 0.6 wt.%) which is also reflected in the very low abundance of hydrous minerals in CWNs. The composition of partly crystallized inclusions is evidence that the high peralkalinity and enrichment in Fe of this melt was favorable to the crystallization of minerals rich in alkalis and Fe and poor in Al. The deficiency in Al is clearly expressed in the crystallization of aluminosilicates (delhayelite, leucite, tetraferriannite, K-feldspar, nepheline, sodalite) containing high tetrahedral  $\text{Fe}^{3+}$ , and in the appearance of Al-poor aegirine-rich clinopyroxene and Al-free Ba–Sr–Ti-rich silicates such as barytolamprophyllite or a mineral of the shcherbakovite–noonkanbahite–batisite series. This tendency is traced both in nepheline-hosted inclusions (our data) and in the groundmass of the Lengai CWNs (Dawson, 1998; Dawson and Hill, 1998; Klaudius and Keller, 2006). In general, such evolution did not lead to increasing peralkalinity for residual portions of silicate melt. It should be also noted again that during cooling and crystallization, the silicate melt may have exchanged some mobile elements with coexisting natrocarbonatite liquid.

## 9. Summary

Despite the extensive compositional data presented here for mineral-hosted inclusions in our 1917 CWN, we obtained more information from our heating experiments. Firstly, the data showed the existence of high temperature ( $900\text{--}1130^\circ\text{C}$  and higher) silicate–

natrocarbonatite immiscibility in a carbonated nephelinite magma that probably occurred in an intermediate chamber. Secondly, we show a possible path for further evolution of natrocarbonatite melt with decreasing temperature. Of course, the questions about the position of an intermediate chamber (shallow depths or deeper?) and the composition of the pre-immiscible parental magma are still open because our microthermometric studies do not allow the estimations of the pressure and composition for the early stage of the initial magma. Unfortunately, the coexistence of immiscible silicate and natrocarbonatite melts over a very wide temperature range ( $1130\text{--}600^\circ\text{C}$ ) does not give a direct answer about PT-conditions when natrocarbonatite liquid was totally separated from silicate magma to form individual eruptions.

In general, the continued evolution of a natrocarbonatite melt after liquid immiscibility and its relations with coexisting silicate magma needs more detailed studies, in particularly in the case of silicate–melt inclusions with numerous carbonate globules. Such investigations will resolve whether individual carbonate globules in silicate glass have different or identical compositions and whether they should be in equilibrium with silicate melt and minerals as suggested by Mitchell (2009) and Guzmics et al. (2011), based on melt inclusions and experimental data. The melt inclusions studies for the Oldoinyo Lengai rocks (Mitchell, 2009; Mitchell and Dawson, 2012-this volume; Sharygin et al., 2009; this work) have shown that the natrocarbonatite–silicate liquid immiscibility is common in the crystallization of CWNs from all eruptions different in age. However, the ratios of different components (carbonate, fluoride, chloride, etc.) in the exsolved natrocarbonatite blebs from different eruptions also need to be studied in details.

## Acknowledgments

The first author thanks L.N. Pospelova, E.N. Nigmatulina, A.T. Titov and N.S. Karmanov for help in microprobe and scanning microscope data of melt inclusions and minerals at the IGM. The authors are grateful to S.G. Simakin and E.V. Potapov (Yaroslavl) for SIMS data on glasses of nepheline-hosted inclusions in CWN. We thank J. Keller (Freiburg) for consulting in eruption time of the studied CWN, A.A. Zolotarev (St. Petersburg) for X-ray single crystal data for the Lengai CWN wollastonite and I.V. Pekov (Moscow) for help in the identification of a Ba–Ti-rich silicate. The manuscript was improved based on comments and suggestions from reviewers Alan Cooper and Nelson Eby. This work was supported by the Russian Foundation for Basic Research (grant 11-05-00875 to VVS) and funding from the Australian Research Council (Discovery grant DP1092823) and University of Tasmania to VSK and the Alexander von Humboldt Stiftung to ANZ.

## References

- Armbruster, T., Richards, R.P., Gnos, E., Pettko, T., Herwegh, M., 2007. Unusual fibrous sodian tainiolite on phlogopite from marble xenoliths of Mont Saint-Hilaire, Québec, Canada. *The Canadian Mineralogist* 45, 541–549.
- Bagdasaryan, G.P., Gerasimovskiy, V.I., Polyakov, A.I., Gukasyan, R.K., Vernadskiy, V.I., 1973. Age of volcanic rocks in the rift zones of East Africa. *Geokhimiya* 10, 66–71.
- Bazarova, T.Yu., Bakumenko, I.T., Kostyuk, V.P., Panina, L.I., Sobolev, V.S., Chepurov, A.I., 1975. Magmatic Crystallization Based on the Study of Melt Inclusions. *Nauka, Novosibirsk* (in Russian).
- Bell, K., Dawson, J.B., 1995. Nd and Sr isotope systematics of the active Carbonatite Volcano, Oldoinyo Lengai. In: Bell, K., Keller, J. (Eds.), *Carbonatite Volcanism, Oldoinyo Lengai and the Petrogenesis of Natrocarbonatites*. : IAVCEI Proceedings in Volcanology, vol. 4. Springer Verlag, Berlin, pp. 100–112.
- Brooker, R.A., Kjarsgaard, B.A., 2011. Silicate–carbonate liquid immiscibility and phase relations in the system  $\text{SiO}_2\text{--Na}_2\text{O--Al}_2\text{O}_3\text{--CaO--CO}_2$  at 0.1–2.5 GPa with applications to carbonatite genesis. *Journal of Petrology* 52, 1281–1305.
- Church, A.A., Jones, A.P., 1995. Silicate–carbonate immiscibility at Oldoinyo Lengai. *Journal of Petrology* 36, 869–889.
- Cooper, A.F., Gittins, J., Tuttle, O.F., 1975. The system  $\text{Na}_2\text{CO}_3\text{--K}_2\text{CO}_3\text{--CaCO}_3$  at 1 kbar and its significance in carbonatite petrogenesis. *American Journal of Science* 275, 534–560.
- Dawson, J.B., 1962. The geology of Oldoinyo Lengai. *Bulletin of Volcanology* 24, 349–387.

- Dawson, J.B., 1989. Sodium carbonate lavas from Oldoinyo Lengai, Tanzania: implications for carbonatite complex genesis. In: Bell, K. (Ed.), *Carbonatites – Genesis and Evolution*. In: Hyman, London, pp. 255–277.
- Dawson, J.B., 1998. Peralkaline nephelinite–natrocarbonatite relationships at Oldoinyo Lengai, Tanzania. *Journal of Petrology* 39, 2077–2094.
- Dawson, J.B., 2008. The Gregory rift valley and Neogene–Recent volcanoes of northern Tanzania. Geological Society London Memoir (33), 98.
- Dawson, J.B., Hill, P.G., 1998. Mineral chemistry of a peralkaline combeite lamprophyllite nephelinite from Oldoinyo Lengai, Tanzania. *Mineralogical Magazine* 62, 179–196.
- Dawson, J.B., Keller, J., Nyamweru, C., 1995a. Historic and recent eruptive activity of Oldoinyo Lengai. In: Bell, K., Keller, J. (Eds.), *Carbonatite Volcanism, Oldoinyo Lengai and the Petrogenesis of Natrocarbonatites*. : IAVCEI Proceedings in Volcanology, vol. 4. Springer Verlag, Berlin, pp. 4–22.
- Dawson, J.B., Smith, J.V., Steele, I.M., 1995b. Petrology and mineral chemistry of plutonic igneous xenoliths from the carbonatite volcano, Oldoinyo Lengai, Tanzania. *Journal of Petrology* 36, 797–826.
- Dawson, J.B., Pyle, D.M., Pinkerton, H., 1996. Evolution of natrocarbonatite from a wollastonite nephelinite parent: evidence from the June 1993 eruption of Oldoinyo Lengai, Tanzania. *Journal of Geology* 104, 41–54.
- Donaldson, C.H., Dawson, J.B., Kanaris-Sotiropoulos, R., Batchelor, R.A., Walsh, J.N., 1987. The silicate lavas of Oldoinyo Lengai, Tanzania. *Neues Jahrbuch für Mineralogie. Abhandlungen* 156, 247–279.
- Foster, A., Ebinger, C., Mbede, E., Rex, D., 1997. Tectonic development of the northern Tanzanian sector of the East African Rift System. *Journal of the Geological Society of London* 154, 689–700.
- Genge, M.J., Balme, M., Jones, A.P., 2001. Salt-bearing fumarole deposits in the summit crater of Oldoinyo Lengai, northern Tanzania: interaction between natrocarbonatite lava and meteoric water. *Journal of Volcanology and Geothermal Research* 106, 111–122.
- Golovin, A.V., Sharygin, V.V., Pokhilenko, N.P., 2007. Melt inclusions in olivine phenocrysts in unaltered kimberlites from the Udachnaya–East pipe, Yakutia: some aspects of kimberlite magma evolution during late crystallization stages. *Petrology* 15, 168–183.
- Guzmics, T., Mitchell, R.H., Szabo, C., Berkesi, M., Milke, R., Abart, R., 2011. Carbonatite melt inclusions in coexisting magnetite, apatite and monticellite in Kerimasi calcicarbonatite, Tanzania: melt evolution and petrogenesis. *Contributions to Mineralogy and Petrology* 161, 177–196.
- Halama, R., McDonough, W.F., Rudnick, R.L., Keller, J., Klaudius, J., 2007. The Li isotopic composition of Oldoinyo Lengai: nature of the mantle sources and lack of isotopic fractionation during carbonatite petrogenesis. *Earth and Planetary Science Letters* 254, 77–89.
- Hamilton, D.H., Freestone, I.C., Dawson, J.B., Donaldson, C.H., 1979. Origin of carbonatites by liquid immiscibility. *Nature* 279, 52–54.
- Jago, B.C., 1991. The role of fluorine in the evolution of alkali-bearing carbonatite magma and the formation of carbonatite-hosted apatite and pyrochlore deposits. PhD thesis, University of Toronto, Ontario, Canada.
- Jago, B.C., Gittins, J., 1991. The role of fluorine in carbonatite magma evolution. *Nature* 349 (6304), 56–58.
- Jochum, K.P., Dingwell, D.B., Rocholl, A., Stoll, B., Hofmann, A.W., Becker, S., Besmehn, A., Bessette, D., Dietze, H.-J., Dulski, P., Erzinger, J., Hellebrand, E., Hoppe, P., Horn, I., Janssens, K., Jenner, G., Klein, M., McDonough, W.F., Maetz, M., Mezger, K., Münker, C., Nikogosian, I.K., Pickhart, C., Raczek, I., Rhede, D., Seufert, H.M., Simakin, S.G., Sobolev, A.V., Spettel, A.V., Straub, S., Vincze, L., Wallianos, A., Weckwerth, G., Weyer, S., Wolf, D., Zimmer, M., 2000. The preparation and preliminary characterisation of eight geological MPI-DING reference glasses for in-situ microanalysis. *Geostandard Newsletter – The Journal of Geostandards and Geoanalysis* 24, 87–133.
- Kamenetsky, V.S., Kamenetsky, M.B., Sharygin, V.V., Faure, K., Golovin, A.V., 2007. Chloride and carbonate immiscible liquids at the closure of the kimberlite magma evolution (Udachnaya–East kimberlite, Siberia). *Chemical Geology* 237, 384–400.
- Keller, J., Krafft, M., 1990. Effusive natrocarbonatite activity of Oldoinyo Lengai, June 1988. *Bulletin of Volcanology* 52, 629–645.
- Keller, J., Spettel, B., 1995. The trace element composition and petrogenesis of natrocarbonatites. In: Bell, K., Keller, J. (Eds.), *Carbonatite Volcanism: Oldoinyo Lengai and the Petrogenesis of Natrocarbonatites*. : IAVCEI Proceedings in Volcanology, vol. 4. Springer Verlag, Berlin, pp. 70–86.
- Keller, J., Zaitsev, A., Wiedenmann, D., 2006. Primary magmas at Oldoinyo Lengai: the role of olivine melilitites. *Lithos* 91, 150–172.
- Keller, J., Klaudius, J., Kervyn, M., Ernst, G.G.J., Mattsson, H.B., 2010. Fundamental changes in the activity of the natrocarbonatite volcano Oldoinyo Lengai, Tanzania. I. New magma composition during the 2007–2008 explosive eruptions. *Bulletin of Volcanology* 72, 893–912.
- Kervyn, M., Ernst, G.G.J., Keller, J., Vaughan, R.G., Klaudius, J., Pradal, E., Belton, F., Mattsson, H.B., Mbede, E., Jacobs, P., 2010. Fundamental changes in the activity of the natrocarbonatite volcano Oldoinyo Lengai, Tanzania. II. Eruptive behaviour during the 2007–2008 explosive eruptions. *Bulletin of Volcanology* 72, 912–931.
- Kjarsgaard, B.A., Peterson, T.D., 1991. Nephelinite–carbonatite liquid immiscibility at Shombole volcano, East Africa: petrographic and experimental evidence. *Mineralogy and Petrology* 43, 293–314.
- Kjarsgaard, B.A., Hamilton, D.L., Peterson, T.D., 1995. Peralkaline nephelinite/carbonatite liquid immiscibility: comparison of phase composition in experiments and natural lavas from Oldoinyo Lengai. In: Bell, K., Keller, J. (Eds.), *Carbonatite Volcanism: Oldoinyo Lengai and the Petrogenesis of Natrocarbonatites*. : IAVCEI Proceedings in Volcanology, vol. 4. Springer Verlag, Berlin, pp. 163–190.
- Klaudius, J., Keller, J., 2006. Peralkaline silicate lavas at Oldoinyo Lengai, Tanzania. *Lithos* 91, 173–190.
- Lee, W.J., Wyllie, P.J., 1994. Experimental data bearing on liquid immiscibility, crystal fractionation, and the origin of calcicarbonatites and natrocarbonatites. *International Geology Review* 36, 797–819.
- Lee, W.J., Wyllie, P.J., 1998. Processes of crustal carbonatite formation by liquid immiscibility and differentiation, elucidated by model systems. *Journal of Petrology* 39, 2005–2015.
- MacIntyre, R.M., Dawson, J.B., Mitchell, J.G., 1974. Age of fault movements in the Tanzania sector of the East African Rift system. *Nature* 247, 354–356.
- Mattsson, H.B., Reusser, E., 2010. Mineralogical and geochemical characterization of ashes from an early phase of the explosive September 2007 eruption of Oldoinyo Lengai (Tanzania). *Journal of African Earth Sciences* 58, 752–763.
- Mazzi, F., Galli, E., Gottardi, G., 1976. The crystal structure of tetragonal leucite. *American Mineralogist* 61, 108–115.
- McDonough, W.F., Sun, S.S., 1995. Composition of the Earth. *Chemical Geology* 120, 223–253.
- Mitchell, R.H., 1997. Carbonate–carbonate immiscibility, neighborite and potassium iron sulphide in Oldoinyo Lengai natrocarbonatite. *Mineralogical Magazine* 61, 779–789.
- Mitchell, R.H., 2006a. Sylvite and fluorite microcrysts, and fluorite–nyerereite intergrowths from natrocarbonatite, Oldoinyo Lengai, Tanzania. *Mineralogical Magazine* 70, 103–114.
- Mitchell, R.H., 2006b. Mineralogy of stalactites formed by subaerial weathering of natrocarbonatite hornitos at Oldoinyo Lengai, Tanzania. *Mineralogical Magazine* 70, 437–444.
- Mitchell, R.H., 2009. Peralkaline nephelinite–natrocarbonatite immiscibility and carbonatite assimilation at Oldoinyo Lengai, Tanzania. *Contributions to Mineralogy and Petrology* 158, 589–598.
- Mitchell, R.H., Belton, F., 2004. Nicalite–cuspidine solid solution and manganese monticellite from natrocarbonatite, Oldoinyo Lengai, Tanzania. *Mineralogical Magazine* 68, 787–799.
- Mitchell, R.H., Dawson, J.B., 2007. The 24th September 2007 ash eruption of the carbonatite volcano Oldoinyo Lengai, Tanzania: mineralogy of the ash and implications for formation of a new hybrid magma type. *Mineralogical Magazine* 71, 483–492.
- Mitchell, R.H., Dawson, J.B., 2012. Carbonate–silicate immiscibility and extremely peralkaline silicate glasses at Oldoinyo Lengai volcano, Tanzania. *Lithos* 152, 40–46 (this volume).
- Mitchell, R.H., Kjarsgaard, B.A., 2008. Experimental studies of the system  $\text{Na}_2\text{Ca}(\text{CO}_3)_2\text{–NaCl–KCl}$  at 0.1 GPa: implications for the differentiation and low-temperature crystallization of natrocarbonatite. *The Canadian Mineralogist* 46, 971–980.
- Mitchell, R.H., Kjarsgaard, B.A., 2011. Experimental studies of the system  $\text{Na}_2\text{CO}_3\text{–CaCO}_3\text{–MgF}_2$  at 0.1 GPa: implications for the differentiation and low-temperature crystallization of natrocarbonatite. *Journal of Petrology* 52, 1265–1280.
- Naumov, V.B., Polyakov, A.I., Romanchev, B.P., 1972. Crystallization conditions for volcanic rocks from East Africa rift zones suggested by thermobarometric studies. *Geokhimiya* 6, 663–668.
- Nielsen, T.F.D., Veksler, I.V., 2002. Is natrocarbonatite a cognate fluid condensate? Contributions to Mineralogy and Petrology 142, 425–435.
- Panina, L.I., 2005. Multiphase carbonate–salt immiscibility in carbonatite melts: data on melt inclusions from the Krestovskiy massif minerals (Polar Siberia). Contributions to Mineralogy and Petrology 150, 19–36.
- Pekov, I.V., Chukanov, N.V., Ferraris, G., Ivaldi, G., Pushcharovsky, D.Yu., Zadov, A.E., 2003. Shirokshinite,  $\text{K}(\text{NaMg}_2)\text{Si}_4\text{O}_{10}\text{F}_2$ , a new mica with octahedral Na from Khibiny massif, Kola Peninsula: descriptive data and structural disorder. *European Journal of Mineralogy* 15, 447–454.
- Pekov, I.V., Zubkova, N.V., Chukanov, N.V., Sharygin, V.V., Pushcharovsky, D.Yu., 2009. Crystal chemistry of delhayelite and hydrodelhayelite. *Doklady Earth Sciences* 428, 1216–1221.
- Peterson, T.D., 1989a. Peralkaline nephelinites: I. Comparative petrology of Shombole and Oldoinyo Lengai, East Africa. Contributions to Mineralogy and Petrology 101, 458–478.
- Peterson, T.D., 1989b. Peralkaline nephelinites: II. Low pressure fractionation and the hypersodic lavas of Oldoinyo Lengai. Contributions to Mineralogy and Petrology 102, 336–346.
- Peterson, T.D., 1990. Petrology and genesis of natrocarbonatite. Contributions to Mineralogy and Petrology 105, 143–155.
- Peterson, T.D., Kjarsgaard, B.A., 1995. What are the parental magmas at Oldoinyo Lengai? In: Bell, K., Keller, J. (Eds.), *Carbonatite Volcanism: Oldoinyo Lengai and the Petrogenesis of Natrocarbonatites*. : IAVCEI Proceedings in Volcanology, vol. 4. Springer Verlag, Berlin, pp. 70–86.
- Rankin, A.H., Le Bas, M.J., 1974. Liquid immiscibility between silicate and carbonate melts in naturally-occurring ijolite magmas. *Nature* 250, 206–209.
- Romanchev, B.P., 1972. Formation conditions for rocks of some carbonatite complexes of Eastern Africa based on thermometry of inclusions. *Geokhimiya* 2, 172–179 (in Russian).
- Sharygin, V.V., Kamenetsky, V.S., Zaitsev, A.N., Kamenetsky, M.B., 2009. Immiscible melt inclusions in nepheline phenocrysts from nephelinites lavas, Oldoinyo Lengai: heating experiments and compositional constraints. In: Kogarko, L.N. (Ed.), Abstracts of XXVI International conference, School «Geochemistry of Alkaline rocks», Moscow, Russia, pp. 136–138. <http://alkaline.web.ru/2009/Sharygin2.htm>.
- Sharygin, V.V., Zaitsev, A.N., Starikova, A.Ye., 2010. Silicate–melt inclusions in minerals of ijolite xenoliths, Oldoinyo Lengai volcano, Tanzania. In: Sharygin, V.V. (Ed.), ACROFI-III and TBG XIV Abstracts Volume, Novosibirsk, Russia, pp. 206–207. <http://acrofi.igm.nsc.ru>.
- Sharygin, V.V., Zhitova, L.M., Nigmatullina, E.N., 2011. Fairchildite  $\text{K}_2\text{Ca}(\text{CO}_3)_2$  in phosphorites from Phalaborwa, South Africa: first occurrence in alkaline carbonatite complexes. *Russian Geology and Geophysics* 52, 208–219.
- Simonetti, A., Bell, K., Shady, C., 1997. Trace and rare-earth-element geochemistry of the June 1993 natrocarbonatite lavas, Oldoinyo Lengai (Tanzania). Implications

- for the origin of carbonatite magmas. *Journal of Volcanology and Geothermal Research* 75, 89–106.
- Sobolev, A.V., Slutsky, A.B., 1984. Composition and crystallization conditions of initial melt of the Siberian meimechites in relation to the general problem of the ultrabasic magmas. *Geologiya i Geofizika (Soviet Geology and Geophysics)* 25, 93–104.
- Stoppa, F., Sharygin, V.V., Cundari, A., 1997. New mineral data from the kamafugite–carbonatite association: the melilitolite of Pian di Celle, Italy. *Mineralogy and Petrology* 61, 27–45.
- Stoppa, F., Jones, A.P., Sharygin, V.V., 2009. Nyerereite from carbonatitic rocks at Vulturno volcano: implications for mantle metasomatism and petrogenesis of alkali carbonate melts. *Central European Journal of Geosciences* 1, 131–151.
- Uvarova, Y.A., Sokolova, E., Hawthorne, F.C., Liferovich, R.P., Mitchell, R.H., Pekov, I.V., Zadov, A.E., 2010. Noonkanbahite,  $\text{BaKNaTi}_2(\text{Si}_4\text{O}_{12})\text{O}_2$ , a new mineral species: description and crystal structure. *Mineralogical Magazine* 74, 441–450.
- Veksler, I.V., Nielsen, T.F.D., Sokolov, S.V., 1998. Mineralogy of crystallized melt inclusions from Gardiner and Kovdor ultramafic alkaline complexes: implications for carbonatite genesis. *Journal of Petrology* 39, 2015–2031.
- Veksler, I.V., Dorfman, A.M., Dulski, P., Kamenetsky, V.S., Danyushevsky, L.V., Jeffries, T., Dingwell, D.B., 2012. Partitioning of elements between silicate melt and immiscible fluoride, chloride, carbonate, phosphate and sulfate melts with implications to the origin of natrocarbonatite. *Geochimica et Cosmochimica Acta* 79, 20–40.
- Williams, R.W., Gill, J.B., Bruland, K.W., 1986. Ra–Th disequilibria systematics: time-scale of carbonatite magma formation at Oldoinyo Lengai volcano, Tanzania. *Geochimica et Cosmochimica Acta* 50, 1249–1259.
- Zaitsev, A.N., 2010a. Nyerereite from calcite carbonatite at the Kerimasi volcano, northern Tanzania. *Geology of Ore Deposits* 52 (7), 630–640.
- Zaitsev, A.N., 2010a. Mineralogy, geochemistry and post-crystallization transformation volcanic carbonatites of Gregory Rift (Eastern Africa). Dissertation of Doctor of Science, SPSU, Saint Petersburg (in Russian).
- Zaitsev, A.N., Keller, J., 2006. Mineralogical and chemical transformation of Oldoinyo Lengai natrocarbonatites, Tanzania. *Lithos* 91, 191–207.
- Zaitsev, A.N., Keller, J., Spratt, J., Perova, E.N., Kearsley, A., 2008. Nyerereite–pirssonite–calcite–shortite relationships in altered natrocarbonatites, Oldoinyo Lengai, Tanzania. *The Canadian Mineralogist* 46, 843–860.
- Zaitsev, A.N., Keller, J., Spratt, J., Jeffries, T.E., Sharygin, V.V., 2009. Chemical composition of nyerereite and gregoryite from natrocarbonatites of Oldoinyo Lengai volcano, Tanzania. *Geology of Ore Deposits* 51 (7), 608–616.
- Zaitsev, A.N., Wenzel, T., Spratt, J., Williams, T.C., Strekopytov, S., Sharygin, V.V., Petrov, S.V., Golovina, T.A., Zaitseva, E.O., Markl, G., 2011. Was Sadiman volcano a source for the Laetoli footprint tuff? *Journal of Human Evolution* 61, 121–124.
- Zaitsev, A.N., Marks, M.A.W., Wenzel, T., Spratt, J., Sharygin, V.V., Strekopytov, S., Markl, G., 2012. Mineralogy, geochemistry and petrology of the nephelinitic Sadiman volcano, Crater Highlands, Tanzania. *Lithos* 152, 66–83 (this volume).